frontiers in Marine Science

ORIGINAL RESEARCH
published: 06 June 2018
doi: 10.3389/fmars.2018.00199

Algal Colonization of Young Arctic Sea Ice in Spring

Hanna M. Kauko[1,2], Lasse M. Olsen[1], Pedro Duarte[1], Ilka Peeken[3], Mats A. Granskog[1], Geir Johnsen[4,5], Mar Fernández-Méndez[1], Alexey K. Pavlov[1], Christopher J. Mundy[6] and Philipp Assmy[1]*

[1] Norwegian Polar Institute, Fram Centre, Tromsø, Norway, [2] Trondheim Biological Station, Department of Biology, Norwegian University of Science and Technology, Trondheim, Norway, [3] Alfred Wegener Institute Helmholtz Centre for Polar and Marine Research, Bremerhaven, Germany, [4] Centre for Autonomous Marine Operations and Systems, Trondheim Biological Station, Department of Biology, Norwegian University of Science and Technology, Trondheim, Norway, [5] University Centre in Svalbard, Longyearbyen, Norway, [6] Centre for Earth Observation Science, University of Manitoba, Winnipeg, MB, Canada

The importance of newly formed sea ice in spring is likely to increase with formation of leads in a more dynamic Arctic icescape. We followed the ice algal species succession in young ice (≤0.27 m) in spring at high temporal resolution (sampling every second day for 1 month in May–June 2015) in the Arctic Ocean north of Svalbard. We document the early development of the ice algal community based on species abundance and chemotaxonomic marker pigments, and relate the young-ice algal community to the communities in the under-ice water column and the surrounding older ice. The seeding source seemed to vary between algal groups. Dinoflagellates were concluded to originate from the water column and diatoms from the surrounding older ice, which emphasizes the importance of older ice as a seeding source over deep oceanic regions and in early spring when algal abundance in the water column is low. In total, 120 taxa (80 identified to species or genus level) were recorded in the young ice. The protist community developed over the study period from a ciliate, flagellate, and dinoflagellate dominated community to one dominated by pennate diatoms. Environmental variables such as light were not a strong driver for the community composition, based on statistical analysis and comparison to the surrounding thicker ice with low light transmission. The photoprotective carotenoids to Chl *a* ratio increased over time to levels found in other high-light habitats, which shows that the algae were able to acclimate to the light levels of the thin ice. The development into a pennate diatom-dominated community, similar to the older ice, suggests that successional patterns tend toward ice-associated algae fairly independent of environmental conditions like light availability, season or ice type, and that biological traits, including morphological and physiological specialization to the sea ice habitat, play an important role in colonization of the sea ice environment. However, recruitment of ice-associated algae could be negatively affected by the ongoing loss of older ice, which acts as a seeding repository.

Keywords: sea-ice algae, young ice, Arctic, N-ICE2015, pigments, succession

OPEN ACCESS

Edited by:
Janne-Markus Rintala, University of Helsinki, Finland

Reviewed by:
Daria Martynova, Zoological Institute (RAS), Russia
Klaus Martin Meiners, Australian Antarctic Division, Australia

****Correspondence:***
Hanna M. Kauko
hanna.kauko@npolar.no;
hanna.kauko@alumni.helsinki.fi

Specialty section:
This article was submitted to Marine Ecosystem Ecology, a section of the journal Frontiers in Marine Science

Received: *23 March 2018*
Accepted: *18 May 2018*
Published: *06 June 2018*

Citation:
Kauko HM, Olsen LM, Duarte P, Peeken I, Granskog MA, Johnsen G, Fernández-Méndez M, Pavlov AK, Mundy CJ and Assmy P (2018) Algal Colonization of Young Arctic Sea Ice in Spring. Front. Mar. Sci. 5:199. doi: 10.3389/fmars.2018.00199

INTRODUCTION

The Arctic icescape is changing rapidly, which affects the whole marine system (Meier et al., 2014). Primary production or algal species dynamics and habitats are altered for example by a shorter ice season (Arrigo and van Dijken, 2015) and likely by the reduction of multi-year ice (Lange et al., 2017; Olsen et al., 2017b). The sea ice is also more dynamic and vulnerable to wind forcing (Itkin et al., 2017), which can alter the habitat of ice algae. In the Arctic, ice algae contribute to the annual primary production to a varying degree (<1–60%) depending on season and region (Gosselin et al., 1997; Rysgaard and Nielsen, 2006; Fernández-Méndez et al., 2015). Based on modeling, an estimated 7.5% of annual Arctic primary production is attributed to ice algae (Dupont, 2012). Ice algae also constitute a highly concentrated food source early in the growth season (e.g., Søreide et al., 2010), and thus are a crucial part of Arctic marine foodwebs.

Algae are incorporated into sea ice when it forms through, for example, sieving by growing (Syvertsen, 1991; Lund-Hansen et al., 2017) or rising ice crystals (Reimnitz et al., 1990). Waves, currents, vertical mixing, and other physical factors enhance the entrainment: encounter rates between particles and ice crystals are increased by mixing of crystals into water and water movement through forming ice (Weissenberger and Grossmann, 1998) and along irregularities in bottom-ice topography(Krembs et al., 2002; Lund-Hansen et al., 2017). Frazil ice, which is formed under turbulent conditions (Petrich and Eicken, 2010), was observed to have higher foraminifera abundance than congelation ice (Dieckmann et al., 1990). Also active migration of motile species, and growth even under low irradiances contribute to inhabiting the ice and may be important under calm conditions (Melnikov, 1995; Weissenberger, 1998). In field studies, ice formation has been observed to preferentially retain larger cells (Gradinger and Ikävalko, 1998; Riedel et al., 2007; Rózanska et al., 2008). Further, exopolymeric substances produced by the algae make the cell surfaces sticky and may enhance their incorporation into the ice (Meiners et al., 2003; Riedel et al., 2007).

The main sources of algal species in newly formed sea ice are cells in the water column (pelagic), the sea floor (benthic), or the surrounding older ice (sympagic). Some studies have compared sea ice and water column communities during autumn freeze-up and concluded that the communities differ already during the initial phase of ice formation, suggesting that the seeding community was present in the water column only intermittently (Tuschling et al., 2000; Werner et al., 2007; Niemi et al., 2011). Differences in sea ice communities were observed based on proximity to land i.e., benthic habitats (Ratkova and Wassmann, 2005). Olsen et al. (2017b) suggested that multi-year ice can act as a seed repository, harboring algal cells from a previous growing season that can colonize new ice. In a Greenland fjord the bottom ice algal bloom was formed via spring colonization by phytoplankton, facilitated by increased surface roughness in growing ice crystals (Lund-Hansen et al., 2017). The algal assemblage in new sea ice (ice thickness $\leq$0.03 m) from the Beaufort Sea was similar to the one in the water column, but became different in older stages of ice (Rózanska et al., 2008). Both ice melting and freezing seem to trigger increased species exchange between the water column and sea ice (Hardge et al., 2017). Thus the ice algal community apparently can have many origins, but their relative importance for ice algal recruitment is still not well-known.

Community development can be investigated in light of characteristics of the species present and environmental conditions affecting the species. Further, the number of observed species and how evenly abundance is distributed among the species describe communities (Peet, 1974). Succession refers to changes in species composition and abundance over time. Concepts of species succession (reviewed in McCook, 1994) are derived from work with plant and rocky bottom communities and aim to explain the mechanisms that lead to a certain type of community after disturbance of a site, such as modification of the site by early-colonizing species.

Previous sea ice colonization studies of new and young ice have been conducted in autumn or winter, or in mesocosm experiments (see references above). However, with the ongoing changes in the Arctic icescape, new ice formation during the main algal growth season will possibly increase and offer new habitats for the sympagic communities. Contrary to autumn, light intensity increases during spring, and in spring young ice is a high-light environment compared to older ice with thick snow cover (Kauko et al., 2017), or new ice formed in autumn or winter. Algae in general face an ever-fluctuating light climate, altered e.g., by changing cloud and snow covers. To balance incoming irradiance with the capacity of the photosynthetic apparatus, algae need photoacclimation mechanisms such as adjustment of the cellular pigment pool (reviewed in Brunet et al., 2011). In response to increasing irradiance, changes in the fraction of light-harvesting pigments (LHP) and photoprotective carotenoids (PPC) occur. The latter do not channel the absorbed energy to photosynthesis but dissipate it as heat, thus protecting the photosystems from excess light. The ratios of PPCs to LHP give information on physiology and light history of cells. In addition, many LHP are specific to certain algal groups and can serve as a proxy for taxonomic composition (reviewed in Jeffrey et al., 2011), including those of ice algal communities (Alou-Font et al., 2013).

Increasing light availability due to sea ice retreat has been shown to alter phytoplankton dynamics in the Arctic Ocean using ocean color remote sensing (Arrigo and van Dijken, 2015), but similar large-scale studies are not yet possible for the sea ice habitat due to lack of suitable methods. We have made an effort to understand physical and biological processes in a high-light, young sea ice environment in a refrozen lead during Arctic spring. In a previous study, we have shown that the biomass in the young ice in the refrozen lead was similar to the surrounding older and thicker ice while the light climate was very different, and that algae in the young ice had high concentrations of ultraviolet (UV)-protecting pigments (Kauko et al., 2017). In this paper, we investigate the colonization of the young ice by ice algae and how that relates both to the possible seeding sources, and to the light environment and other environmental conditions. We further examine light acclimation by investigating the photoprotective carotenoids synthetized by

the algae. The objectives of the study were to describe the succession of ice algal species and algal pigment concentrations in young sea ice formed in spring, identify the most important drivers for the algal succession, and compare the young ice community with the surrounding older ice and water column to identify the seeding source.

METHODS

Field Sampling

Young ice (thickness 0.17–0.27 m; Petrich and Eicken, 2010) in a recently refrozen lead was sampled during the Norwegian young sea ICE (N-ICE2015) expedition in the pack ice north of Svalbard at 80.5–82.4°N (**Figure 1A**) in spring 2015 (Granskog et al., 2016, 2018). Ice coring was conducted from early May, a few days after ice reformed over the whole lead, to the beginning of June (Supplementary Table 1) when the ice in the lead broke up. Ice cores for biological samples were first collected close to the edge of the lead (4 and 6 May) and thereafter 13 times (7 May−3 June; approximately every second day) along a transect (five coring sites, three cores pooled at each site) toward the center of the lead (**Figure 1B**). On subsequent sampling days, the transect was moved 2–3 m to the side in order to sample undisturbed ice. Ice cores were melted onboard overnight in the dark at room temperature and unbuffered (Rintala et al., 2014). After 18 May, the ice cores were divided into two sections, where the bottom section was always 0.10 m thick and the top section constituted the remaining part of the core (0.09–0.17 m thick). Salinity of the melted ice cores was measured with a WTW Cond 3110 probe (WTW Wissenschaftlich-Technische Werkstätten GmbH, Weilheim, Germany). Brine salinity was calculated from ice temperature (Cox and Weeks, 1986; Leppäranta and Manninen, 1988). The method for ice core stratigraphy studies is described in Olsen et al. (2017b) and based on Lange (1988). Incoming and ice-transmitted planar downwelling spectral irradiance was measured with two Ramses ACC-VIS spectroradiometers (TriOS Mess- und Datentechnik GmbH, Rastede, Germany) for the wavelength range 320–950 nm (irradiance data are available from Taskjelle et al., 2016). Sampling on the lead is described in detail in Kauko et al. (2017) and biochemical and basic physical data can be found in Assmy et al. (2017a). First-year ice (FYI) and second-year ice (SYI) were sampled weekly and melted by the same procedure (Olsen et al., 2017b). Two cores were pooled and the bottom 0.20 m were cut into 0.10 m long sections and the remaining ice core into 0.20 m sections (all SYI and first FYI coring) or two equal sections (rest of FYI). The water column was sampled via CTD rosettes (one operated from the ship and one through a hole on the adjacent ice floe) twice per week (Assmy et al., 2017b).

Laboratory Methods

From the melted ice core sections 190 mL samples were fixed with glutaraldehyde and 20% hexamethylenetetramine-buffered formaldehyde at final concentrations of 0.1 and 1%, respectively. The samples were stored dark and cool in 200 mL brown glass bottles. Sub-samples were settled in 10 mL Utermöhl sedimentation chambers (HYDRO-BIOS©, Kiel, Germany) for 48 h. Subsequently, protists were identified and counted on a Nikon Ti-U inverted light microscope by the Utermöhl method (Edler and Elbrächter, 2010). Cells were counted in transects. At least 50 cells of the dominant species were counted in each sample (error of ±28% according to Edler and Elbrächter, 2010). Microscopy count data can be found in Olsen et al. (2017a). Abundances (cells L^{-1}) were converted to biomass (mg carbon m^{-3}) using biovolume calculations (Hillebrand et al., 1999) and carbon conversion factors (Menden-Deuer and Lessard, 2000).

Additional samples from the melted ice cores were taken to analyze the algal pigment composition, including diagnostic marker pigments and pigments related to the xanthophyll cycle. For this 100–300 mL melted ice was filtered through 25 mm GF/F filters and shock frozen in liquid nitrogen. The samples were stored at −80°C until analysis. Pigments were analyzed by reverse-phase high performance liquid chromatography (HPLC) using a VARIAN Microsorb-MV3 C8 column (4.6 × 100 mm) and HPLC-grade solvents (Merck), a Waters 1,525 binary pump equipped with an auto sampler (OPTIMAS™), a Waters photodiode array detector (2,996) and the EMPOWER software. For further details see Tran et al. (2013). The ice core samples were melted overnight in darkness and therefore the ratios of the pigments involved in the xanthophyll cycle do not strictly resemble the sampling moment, but together represent a pool of photoprotective carotenoids and are here reported as a sum concentration. HPLC data can be found in Assmy et al. (2017a). An overview of marker pigments and chemotaxonomy can be found in Jeffrey et al. (2011), Higgins et al. (2011), and in the data sheets of Roy et al. (2011). A review of pigments involved in the photoacclimation process can be found in Brunet et al. (2011).

Statistical Methods

Statistical analyses were performed with R (R Core Team, 2017). Data from young ice (including all coring sites and vertical sections, 110 samples) were compared to water column data down to 50 m (23 April−4 June, 69 samples from 17 CTD casts) and to data from the surrounding SYI/FYI (all vertical sections, 22 April−5 June, 74 samples from 11 cores).

Non-metric multidimensional scaling (NMDS), performed with the function *isoMDS* in the MASS package (Venables and Ripley, 2002), was used to investigate the algal community similarity between the different environments based on algal abundance (counts). The count data were first square-root transformed and Bray-Curtis dissimilarity was used for the scaling (calculated with the vegan package; Oksanen et al., 2017).

Shannon's diversity indices (H) were calculated for the species count data with the function *diversity* in the vegan package, defined as $H = -\text{sum}\ (p_i \ln p_i)$, where p_i is the proportion of individuals of species i. Pielou's species evenness (J) was calculated as $J = H/H_{max}$, where H_{max} is a maximum diversity index. Further, $H_{max} = \log_2(S)$, where S is the species richness (species number).

To relate the ice algal species abundance in the young ice to environmental variables, canonical correspondence analysis (CCA; suitable for count data) was performed and additionally function *envfit* was used to fit the environmental variables on NMDS analysis of the young ice. Both were performed with the

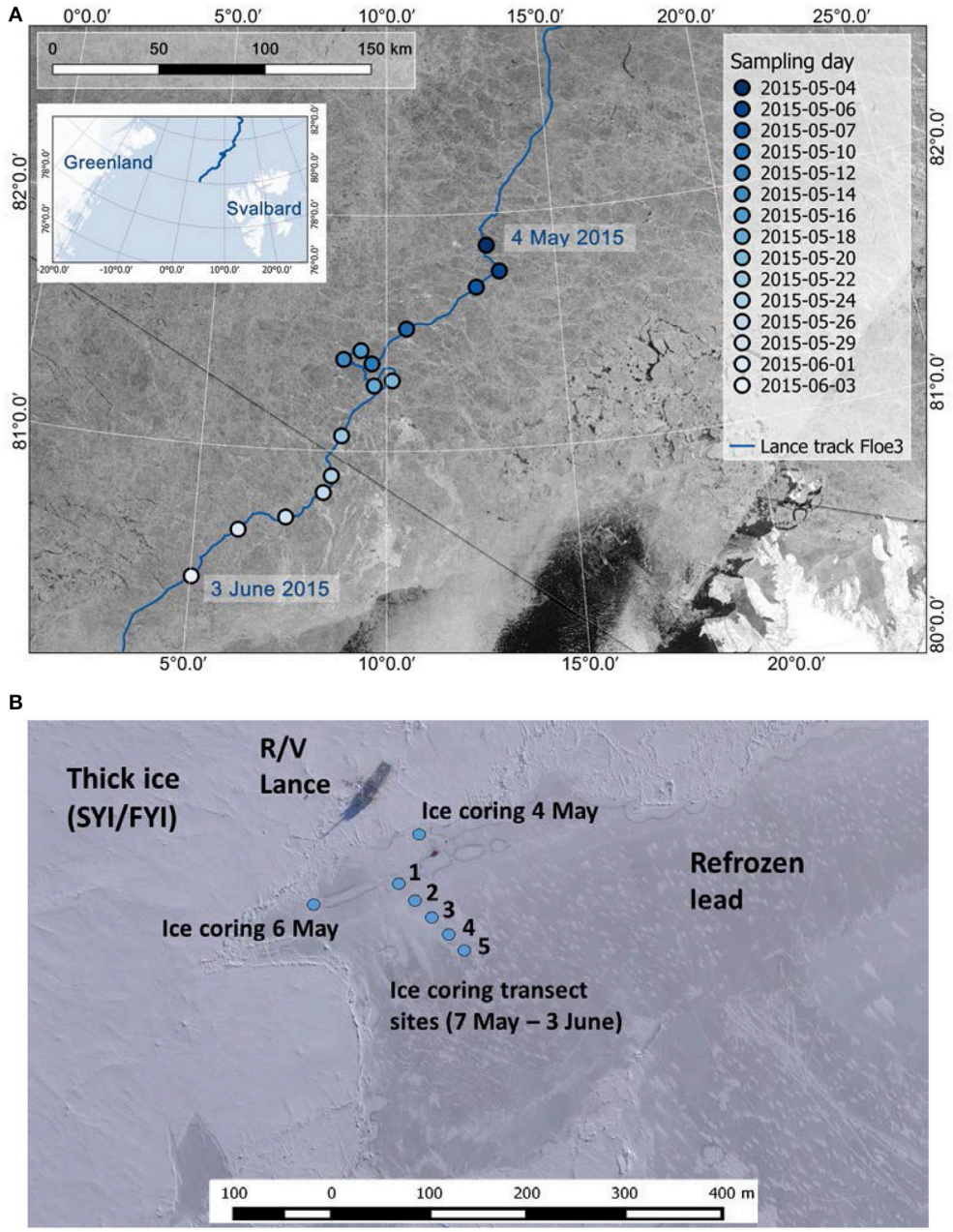

FIGURE 1 | (A) Study area with the drift trajectory of R/V Lance and sampling location on each sampling day. **(B)** Ice coring locations on the young ice in the lead. In **(A)** satellite image (taken on 25 May 2015) source: RADARSAT-2 image provided by NSC/KSAT under the Norwegian-Canadian RADARSAT agreement. RADARSAT-2 Data and Products © MacDonald, Dettwiler and Associates Ltd (2013). All Rights Reserved. RADARSAT is an official mark of the Canadian Space Agency. Map created by the Norwegian Polar Institute/Max König. Aerial image in **(B)** (taken on 23 May 2015): Vasily Kustov and Sergey Semenov (Arctic and Antarctic Research Institute, St. Petersburg, Russia). Maps modified from Kauko et al. (2017).

vegan package and all samples (110) and species were included in the analysis. Environmental variables included snow thickness (indicative also for light intensity) and bulk salinity. Surface water column nitrate concentration (silicate did not change over the sampling period) correlated strongly with bulk salinity of the sea ice and was excluded from further analysis. Bulk salinity therefore also represents the water column nitrate dynamics. There were unfortunately no nutrient samples from the lead ice. Likewise, temperature values, which enable calculation of brine salinity, were not available for the whole period, thus bulk salinity was used. Ice thickness could indicate ice melting events and therefore changes in the physical habitat, but because of strong correlation with snow thickness it was not included in the analysis. The variable snow thickness thus represents several

environmental variables that co-vary, including average in-ice irradiance of the past 48 h, which was calculated for the sampling events. The environmental data were standardized prior to usage by subtracting the mean and then dividing by standard deviation.

The function *anosim* in the vegan package was used to test if variation in the count data was higher between the sampling days than between the ice coring sites on the young ice, to justify the use of averages of the five coring sites.

In time series figures for the days when ice cores were sectioned in two, first a volumetric average of the ice core bottom and top section values (biomass and pigment concentrations) was calculated, and thereafter an average of the five ice coring sites. For 4 and 6 May, averages could be calculated from four and two ice cores, respectively. In the case of pigment to Chl *a* ratios (w: w), the ratio was calculated before averaging the ice core bottom and top sections.

RESULTS

Environmental Conditions

A lead next to the research vessel Lance opened on 23 April. Within the next 3 days, the lead was opening and closing, until it got gradually frozen over by 1 May (width ∼400 m). New ice formed first on the side closest to the vessel, on which the ice coring transect was located. Initially, the edge of the lead was characterized by windblown slush and small ice pieces that congealed to a solid ice cover. By the time of sampling, the ice had reached young ice stage and was thick enough to safely work on. The first ice cores for physical measurements were taken on 1 May at the very edge of the lead (same site as on 4 May; **Figure 1B**). At this site on 1 May, the ice was composed of 0.09 m granular ice in the top half and 0.07 m columnar ice in the bottom. Ice temperatures ranged from −2.0 to −4.2°C and bulk salinities from 9.3 to 10.0. On the site that was sampled on 6 May, the ice consisted of 0.03 m granular ice at the top and 0.14 m columnar ice below. Temperatures ranged from −2.1 to −4.5°C and bulk salinities from 10.3 to 14.9. Brine salinity was up to 78.9 at 0.03 m below the ice core top. For the ice coring transect (7 May onwards; **Figure 1B**), ice structure and other physical properties are reported in detail by Kauko et al. (2017). In short, ice thicknesses ranged from 0.17 to 0.27 m, and increased until 20 May after which a reduction was observed. Sites 2 and 3 had the highest proportion of granular ice (0.17 m on 26 May, compared to 0.05–0.08 m columnar ice) and sites 1 and 5 the lowest (0.04–0.05 m granular ice on 26 May, compared to 0.17–0.195 m columnar ice). Snow thicknesses ranged from 0.01 to 0.06 m. Bulk salinity decreased on average (average of 5 sites) from 7.8 to 5.3 during the sampling period and brine salinities ranged from 23.9 to 52.2 (18 May−1 June). Under-ice downwelling irradiance E_d(PAR) in the photosynthetically active radiation range (PAR, 400–700 nm) was on average 114 μmol photons m^{-2} s^{-1} and ranged from 30 to 350 μmol photons m^{-2} s^{-1} for the period from 12 May to 3 June.

The surrounding ice floe was a composite ice floe consisting of SYI and FYI with a modal ice thickness of 1.2 m and modal snow thickness of 0.45 m (Rösel et al., 2018). Ice temperature and other physical properties are described in Olsen et al. (2017b). Snow depths at the SYI coring site ranged from 0.40 to 0.50 m and at the FYI coring site they were 0.20 m (Olsen et al., 2017b). Irradiance was an order of magnitude lower under FYI than under young ice, and under SYI compared to FYI, with measured irradiances of 0.1–1 μmol photons m^{-2} s^{-1} under SYI and calculated irradiances of 1–20 μmol photons m^{-2} s^{-1} under FYI (Olsen et al., 2017b). Oceanographic conditions of the study area, with Polar Surface Water in the surface, are described in Meyer et al. (2017). Bottom depths during the young ice sampling period varied between 600 and 1,932 m, with shallowest depths occurring toward the end of the study when the ice floe drifted over the Yermak Plateau.

Ice Algal Succession

Temporal Trends in Young Ice

In total, 120 taxa (including e.g., different size categories of flagellates, but excluding cysts) comprising 80 species (including protists identified to species or genus level) were recorded in the young ice samples over the study period. The taxa for all environments are listed in Supplementary Table 2. The community in young ice comprised 54 diatom taxa (45 species), 20 dinoflagellate taxa (15 species), 35 flagellate taxa (15 species), and 11 ciliate taxa (5 species). In this section and section Temporal Trends in Xanthophyll Cycle Pigments, presented values are averages of four ice cores (4 May), two ice cores (6 May), or five coring sites (unless site is specified) where three cores were pooled at each site (transect sampling 7 May onwards; see map in **Figure 1B**). For 18 May and onwards, volumetric averages of ice core bottom and top section values are shown (see section Methods).

In the beginning of the study period, the young ice protist biomass (mg C m^{-3}) and abundance were largely dominated by the ciliate *Mesodinium rubrum* and the cryptophyte chloroplasts (called symbionts hereafter) it had incorporated (**Figure 2** and Supplementary Figure 1). Ciliate cells were presumably damaged during sampling causing release of the symbionts. From 12 May onwards diatoms and dinoflagellates became more prevalent, and together made up almost 70% of the biomass on 12 May. Biomass of ciliates and symbionts decreased thereafter, except on 16 and 20 May. Both flagellates and dinoflagellates biomass increased from early May, but diatoms exponentially increased to over 90% of the total biomass by 3 June, whereas dinoflagellates generally comprised <10% of the biomass. Maximum diatom biomass was 600 mg C m^{-3} on 1 June.

Fucoxanthin, indicative of diatoms, was the most abundant chemotaxonomic marker pigment and increased over the sampling period from 0.01 to 1.26 mg m^{-3} (**Figure 3B**). In terms of marker pigment to Chl *a* ratios, fucoxanthin, and peridinin (a marker for dinoflagellates) showed a contrasting picture during the transect sampling (**Figures 4A,B**). Initially, the peridinin to Chl *a* ratio was high at 0.22 on 7 May, and declined to 0.01 on 1 June. The fucoxanthin to Chl *a* ratio showed the opposite trend, increasing from 0.04 to 0.27.

Species succession was also observed within the diatom community. At the beginning of the transect sampling (7 May onwards) centric diatoms were dominant (**Figure 5A**) and comprised more than 70% of the diatom biomass until

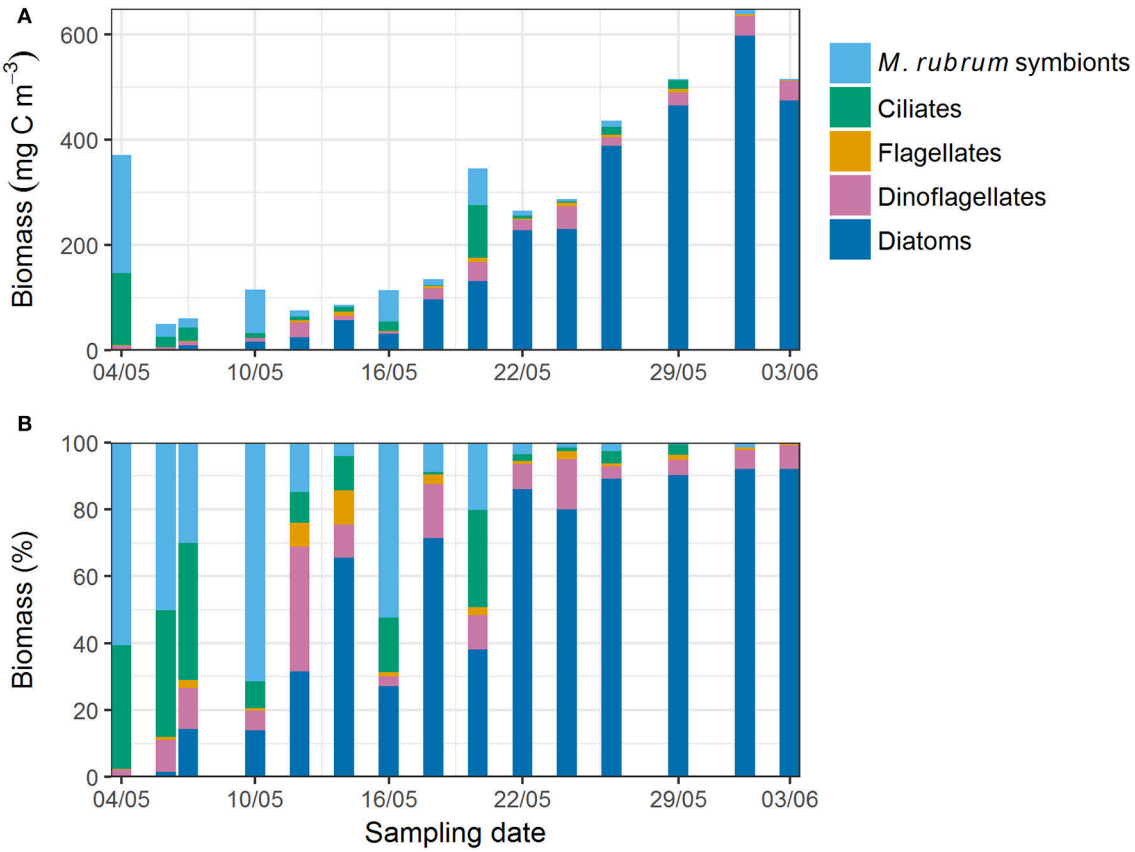

FIGURE 2 | (A) Absolute and **(B)** relative protist biomass in young ice estimated from microscopy counts.

14 May. From 22 May onwards, centric diatoms generally accounted for <60% of diatom biomass, while pennate diatoms increased and dominated (>80% of diatom biomass) from 29 May onwards. The most prevalent taxa among the centric diatoms were *Porosira glacialis* and *Thalassiosira gravida/antarctica* var. *borealis*, and among the pennate diatoms *Nitzschia frigida/neofrigida* (**Figure 6A**), *Fragilariopsis cylindrus* (**Figure 6B**), *Navicula* spp. (**Figure 6C**), and *Pseudo-nitzschia* spp. *Navicula pelagica* appeared in the samples after 18 May. *Fragilariopsis cylindrus* was especially abundant in the middle of the sampling period in terms of cell numbers (Supplementary Figure 2a). On the last two sampling days, *N. frigida/neofrigida* accounted for the highest biomass (ca. 30%) of any individual species.

Cysts accounted for more than 60% of the dinoflagellate biomass on 9 of the 15 sampling days. Cysts of *Polarella glacialis* (**Figure 6E**) occurred throughout the sampling period (**Figure 5B**, Supplementary Figure 2b) and comprised more than 90% of the dinoflagellate biomass on 3 June (35 mg C m^{-3}). Besides cysts, *Gymnodinium* spp. and unidentified dinoflagellates in the size range 10–20 μm were the most prevalent groups among the dinoflagellates.

Unidentified flagellates in the size categories 3–7 and 7–10 μm comprised more than 50% of the flagellate biomass on most sampling days (**Figure 5C**). Prymnesiophytes, consisting of mainly unidentified Coccolithales, peaked on 14 May but were observed on most sampling days. *Phaeocystis pouchetii* was observed from 16 May onwards to a varying degree (biomass <1 mg C m^{-3}). Prasinophytes (**Figure 6F**) and cryptophytes (other than the *M. rubrum* symbionts) were present at low biomass on most sampling days. Chlorophytes were observed only on 4 sampling days. Statocysts of the chrysophyte algae *Dinobryon* sp. were present especially in the latter half of the sampling period (Supplementary Figure 2c).

For Chl *b*, which is found in chlorophytes, prasinophytes, and euglenophytes, concentrations were generally low, up to 0.11 mg m^{-3} on 26 May (**Figure 3D**) and before the transect sampling on 4 May (not shown). The Chl *b* to Chl *a* ratio was highest on 18 May (0.05; **Figure 4C**) and before the coring transect sampling on 6 May (0.07; Supplementary Figure 3c). Alloxanthin (a cryptophyte marker pigment) concentration was at times high: up to 1.72 mg m^{-3} on site 5 on 20 May (**Figure 3E**), and 1.5 mg m^{-3} in one of the ice cores on 4 May. The alloxanthin to Chl *a* ratio was highest on 6 May (Supplementary Figure 3d). Also gyroxanthin diester (found mainly in dinoflagellates) and β,ε-carotene (α-carotene; found in cryptophytes) had marked peaks on site 5 on 20 May (0.15 and 0.84 mg m^{-3}, respectively; **Figures 3F,G**) and before the transect sampling, but otherwise

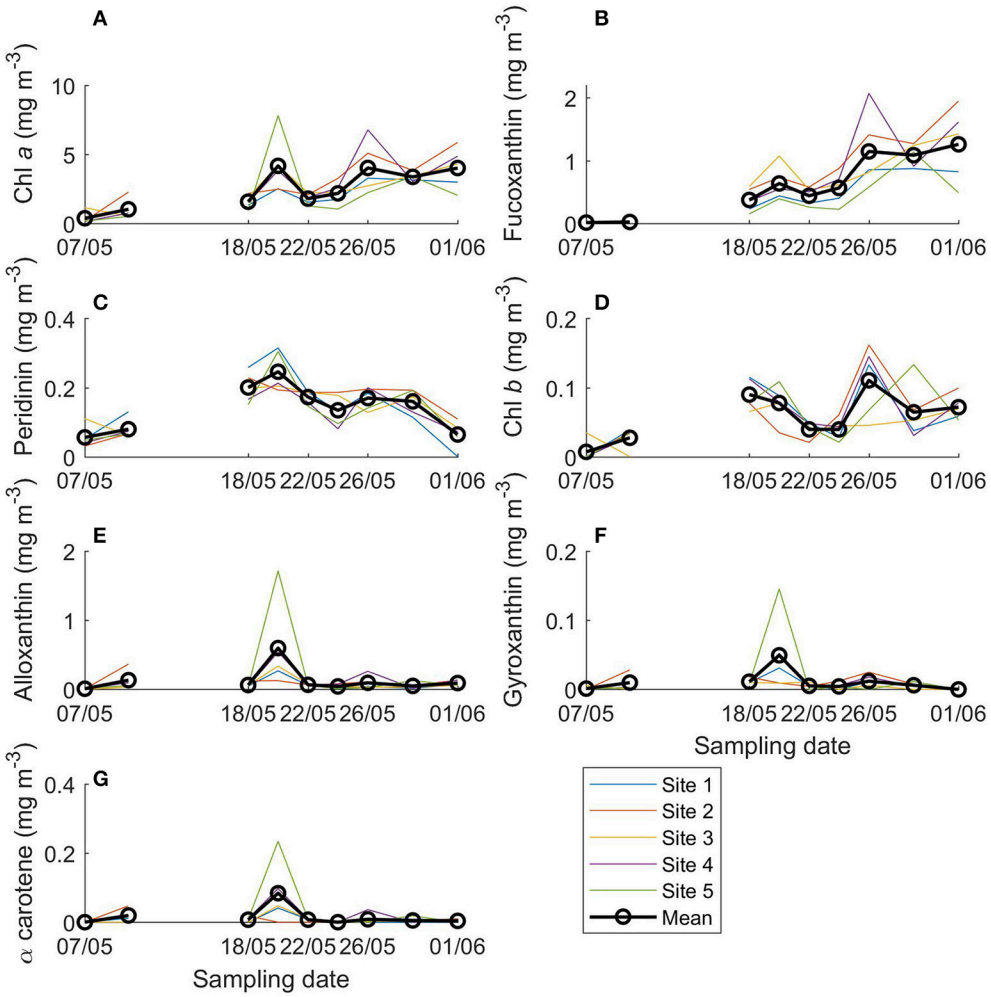

FIGURE 3 | Concentrations of main algal pigments in young ice during the ice coring transect study (7 May onwards). **(A)** Chlorophyll (Chl) *a*, **(B)** fucoxanthin, **(C)** peridinin, **(D)** chlorophyll *b*, **(E)** alloxanthin, **(F)** gyroxanthin diester, and **(G)** α carotene.

had low concentrations during the transect sampling period. The patterns were similar for ratios of these pigments to Chl *a*, but the ratios were low after 24 May (**Figures 4D–F**). Other pigments are shown in Supplementary Figures 4–6 (they were low in concentration or without taxonomic information). No chlorophyll degradation products such as chlorophyllide *a* (algae senescence) or phaeopigments (e.g., phaeophorbide *a*, indicative of grazing) were detected in the samples.

Differences Between Ice Core Bottom and Top Sections in Young Ice

In the previous paragraphs, values were reported for the ice core bottom and top section together (volumetric mean of the values) to be able to investigate the sampling period as a whole (ice core sectioning started on 18 May). In general, abundance and biomass of the species and groups were higher in the ice core bottom sections than in top sections. There were some exceptions, most notably for cysts of the dinoflagellate *Polarella glacialis* and the *Dinobryon* sp. statocysts (**Figure 7**). In terms of relative biomass (Supplementary Figure 7), centric diatoms had a higher contribution in the ice core top sections than in bottom sections. Pennate diatoms had a higher contribution in bottom sections than in top sections, although these also increased and dominated over time in the top sections. For flagellates and dinoflagellates, biomass was low and patterns were not as clear (except for the cysts). Pigment concentrations were likewise in general higher in bottom sections than in top sections. Differences in pigment to Chl *a* ratio between the bottom and top sections are shown in Supplementary Figures 3, 6. Fucoxanthin had higher ratios to Chl *a* in the bottom sections. Gyroxanthin diester, α-carotene, dinoxanthin, and neoxanthin were absent from the top sections, whereas Chl c_3 was only found in top sections.

Comparison of Community Structure Between Habitats

Ice algal community patterns in SYI and FYI are described in Olsen et al. (2017b) and reveal the dominance of pennate

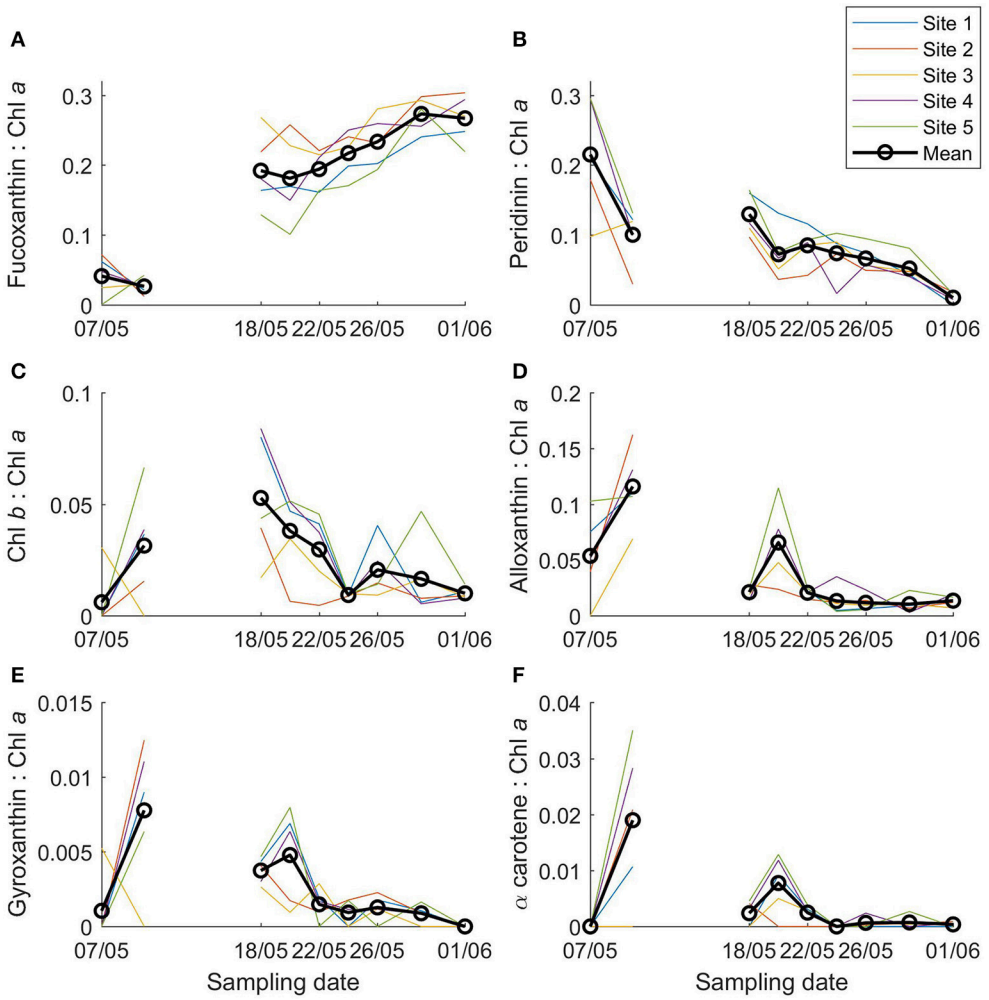

FIGURE 4 | Ratios of main algal pigments to Chl *a* in young ice during the ice coring transect study (7 May onwards). **(A)** Fucoxanthin: Chl *a*, **(B)** peridinin: Chl *a*, **(C)** Chl *b:* Chl *a*, **(D)** alloxanthin: Chl *a*, **(E)** gyroxanthin diester: Chl *a*, and **(F)** α carotene: Chl *a*.

diatoms, especially *N. frigida*, and show that resting cysts were also prominent. In the water column, Chl *a* concentration was low (<0.5 mg m^{-3}) until 25 May when we encountered an under-ice phytoplankton bloom (maximum Chl *a* concentration 7.5 mg m^{-3}) dominated by the haptophyte *P. pouchetii* (Assmy et al., 2017b).

The count data are available in Olsen et al. (2017a). These show that during the early sampling period (22 April−7 May), dinoflagellate abundance in the water column was on average 14-fold higher (average ± standard deviation 1,391 ± 1,217%) compared to diatom abundance. In the surrounding SYI (no FYI sampled at this time period), dinoflagellate abundance was one fourth (24 ± 53%) of diatom abundance. In SYI, 42 diatom, 8 dinoflagellate, and 16 other flagellate taxa (taxonomic level ranging from single species to size categories of flagellates) were identified during this time. In the water column, 8 diatom, 17 dinoflagellate, and 12 other flagellate taxa were identified (Olsen et al., 2017a).

In the early young ice samples (4 May−7 May), 15 diatom (11 of them being pennate species), 12 dinoflagellate, and 9 other flagellate taxa were found, but most taxa were present only in one or two samples. Of these taxa we identified those that were also found in either the water column (samples from 26 April−5 May), SYI (30 April and 7 May) or in both habitats during the re-freezing of the lead and early sampling. Of these, nearly all the dinoflagellates were only found in the water column except for three taxa that were in addition found in four SYI samples. Cysts were found only in SYI and not in the water column. All diatoms were found only in SYI except for two taxa that were also found in one water column sample each, and *N. frigida/neofrigida* in several samples. *N. frigida/neofrigida* was however 1,500 times more abundant in SYI than in the water column.

Temporal Trends in Xanthophyll Cycle Pigments

The photoprotective pigments diadinoxanthin and diatoxanthin increased in both concentration and ratio to Chl *a* over the sampling period, especially compared to the early transect sampling (7 and 10 May; **Figures 8A,C**). The combined concentration increased from 0.01 to 0.87 mg m^{-3} and the ratio

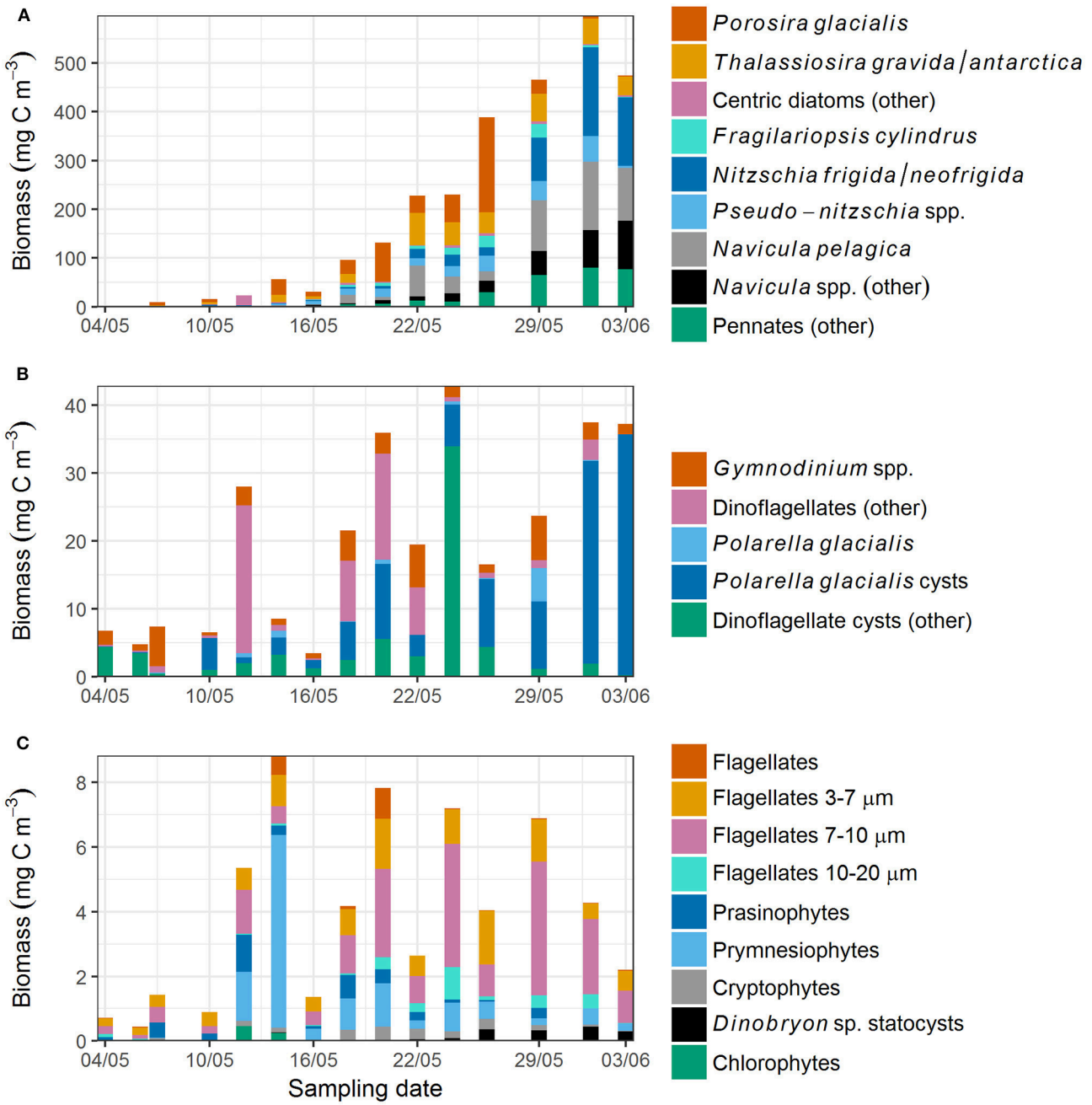

FIGURE 5 | (A) Diatom, **(B)** dinoflagellate, and **(C)** flagellate biomass in young ice. In **(A)**, *Porosira glacialis* and *Thalassiosira gravida/antarctica* are centric diatoms, and the remaining species are pennate diatoms. Note the varying y-axis scale.

of diadinoxanthin+diatoxanthin to Chl *a* from 0.05 to 0.20 over the transect sampling period. Ratios were similar between the ice bottom and top sections (average ± standard deviation for bottom sections 0.19 ± 0.06 and for top sections 0.20 ± 0.07; Supplementary Figure 8a).

Violaxanthin+zeaxanthin concentration and ratio to Chl *a* varied greatly with peaks around 6, 18–20 and 24–29 May (**Figures 8B,D**, Supplementary Figure 8b). The concentration was on average below 0.03 mg m^{-3} and the ratio to Chl *a* was mostly below 0.02.

Statistical Analysis of Community Similarity and Succession

Each habitat—young ice, SYI/FYI, and water column—formed distinct clusters in the NMDS analysis investigating community similarity (**Figure 9**). In the young ice, a temporal shift in species composition is evident (indicated by the coloring) and the samples approach the SYI/FYI group. Ice core bottom and top section samples are on different sides of the young ice samples group (symbols not shown). For thick ice or water column, neither consistent

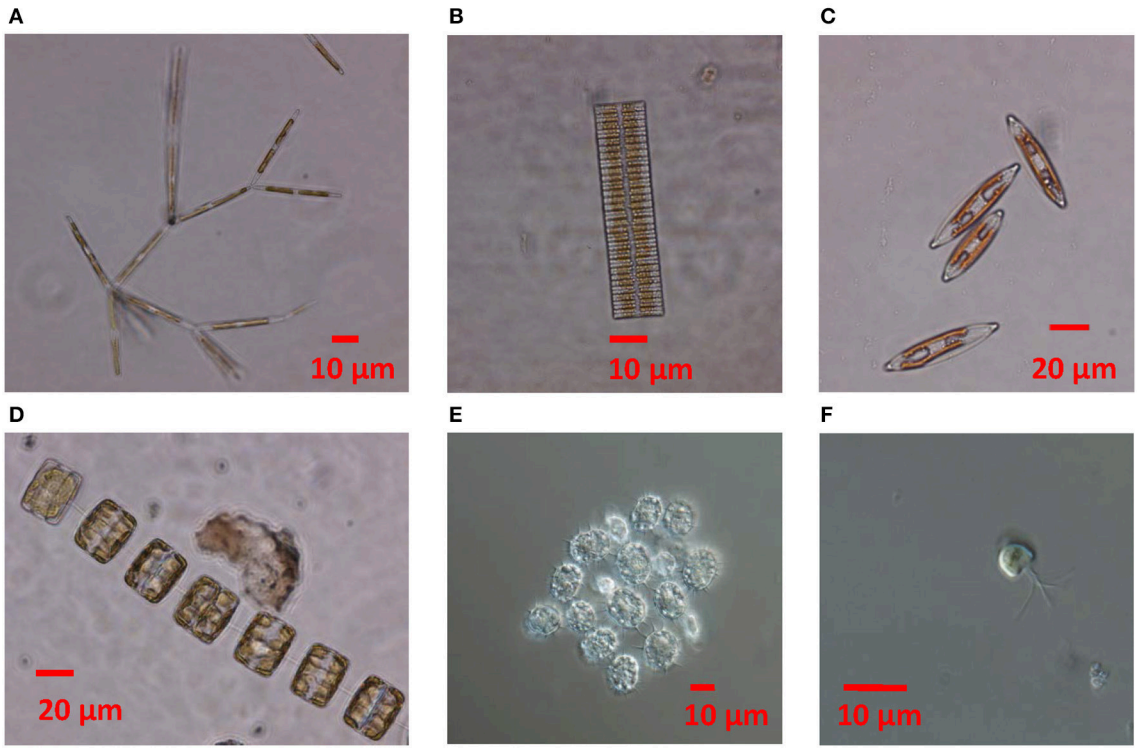

FIGURE 6 | Micrographs showing **(A)** *Nitzschia frigida*, **(B)** *Fragilariopsis cylindrus*, **(C)** *Navicula* sp., **(D)** *Thalassiosira* sp., **(E)** cysts of the dinoflagellate *Polarella glacialis*, **(F)** prasinophyte *Pyramimonas* sp.

vertical (symbols not shown) nor temporal patterns were seen.

The range of Shannon's diversity indices, calculated from species abundance data, was similar in all three environments: 0.01–2.73, 0–2.72, and 0–2.86 for young ice, SYI/FYI and water column, respectively (Supplementary Table 3). When SYI and FYI were treated separately, SYI had a lower diversity range of 0.32–2.46. The young ice had the lowest indices at the beginning of the sampling period whereas the water column samples with lowest diversity were from the latter half of the period (Supplementary Figure 9a). In the SYI/FYI samples, no clear temporal pattern was visible in the diversity index. In general, there was large variation in the indicators (species diversity, richness, and evenness), but species richness increased over time in all habitats (Supplementary Figures 9c,d) and evenness decreased in the water column (Supplementary Figures 9e,f). When the taxon *M. rubrum* symbionts was removed from the dataset (their abundance was likely affected by bursting of *M. rubrum* cells during sampling), evenness had a decreasing trend also in young ice. Furthermore, the early low diversity indices of the young ice disappeared (Supplementary Figure 9b) and the range shifted to 0.84–2.74. Diversity in the young ice was not significantly higher in the ice core top sections than in the bottom sections after removal of the symbionts.

The environmental variables snow thickness and bulk ice salinity (representing several co-varying environmental variables, see section Methods) accounted for 17% of the variance in ice algal abundance in the young ice (CCA in Supplementary Figure 10). The first axis accounted for 16.7% and the second for 0.6% of the variation. The variable bulk salinity aligned close to the first axis and snow thickness close to the second axis. The first axis is parallel to the temporal gradient of the samples (indicated by color in the figure). When the environmental variables were fitted on unconstrained ordination (NMDS for young ice), the patterns were similar and bulk salinity was significantly correlated but snow thickness was not significant.

The sampling days in the young ice differed significantly from each other ($p = 0.001$, $R = 0.41$) for the algal count data, whereas the ice coring sites did not ($p = 0.98$, $R = -0.02$). It is therefore valid to use averages of the coring sites to show the temporal patterns in the young ice biomass and abundance figures.

DISCUSSION

Origin of the Young Ice Community

When new ice forms, cells present in the water column are incorporated into the sea ice. Previous studies have however suggested that not only phytoplankton but also benthic habitats and possibly surrounding ice are sources of ice algae (Ratkova and Wassmann, 2005; Olsen et al., 2017b). In our study, the most probable seeding sources were the water column and surrounding SYI/FYI communities, since the bottom depths at the time of re-freezing were between 1,300 and 2,000 m.

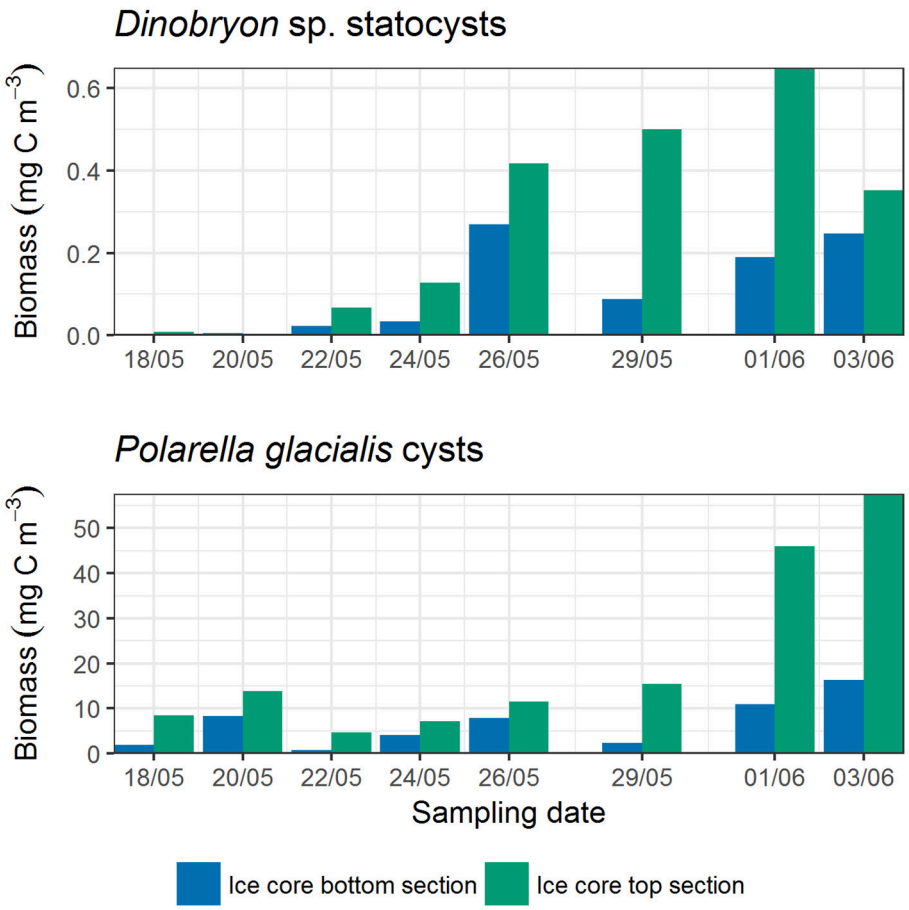

FIGURE 7 | Differences in cyst biomass between ice core bottom and top sections. Ice cores were sectioned from 18 May onwards.

Transport of algae from the shelf waters was not likely as the ice floe was drifting on Polar Surface Water (Meyer et al., 2017). During the re-freezing of the lead and early sampling of the young ice, the algal community in SYI consisted mainly of diatoms and the water column community mainly of dinoflagellates.

The dinoflagellates present in the early young ice samples were in addition found mainly in the water column (and not in SYI). The diatoms, by contrast, were found almost exclusively in SYI except for *N. frigida/neofrigida*. This species is tightly associated with ice, and considering the difference in abundance between SYI and water column, the cells in the water column likely originated from the ice. Olsen et al. (2017b) presented a seeding repository hypothesis for *N. frigida*, suggesting that ice algae from the previous growing season are trapped in the ice and survive over the winter in multi-year ice (MYI), and in the following growing season are able to seed the surrounding new ice. Given our findings, we suggest that the majority of the diatoms in the young ice originated from the surrounding thick ice, although most likely transported via the under-ice water column, while the main source of dinoflagellates was the water column. An additional route for ice-associated species might have been the wind-blown ice pieces that were observed in the lead and were incorporated in the young ice cover. The granular ice that was observed in the ice core top may in turn indicate that the initial ice formed in turbulent conditions, which are favorable for cell harvesting (Dieckmann et al., 1990; Weissenberger and Grossmann, 1998).

In the NMDS analysis each of the habitats (young ice, SYI/FYI, and water column) formed distinct clusters (**Figure 9**). As discussed above, the cells in the young ice are likely to have initially originated from both the water column and older ice. The separation from water column samples means that algae are either selectively incorporated into ice as found in previous studies (Gradinger and Ikävalko, 1998; Riedel et al., 2007; Rózanska et al., 2008), or that community changes happened almost immediately during the first week after ice formation. It was observed that the ice algal community resembled the water column community in new ice ($\leq$0.03 m) but differed in young ice (0.17–0.21 m; Rózanska et al., 2008). Survival in the new habitat may be different; changes for example in salinity and light regime are substantial when moving from the water column to the ice. Brine salinity in the young ice on 6 May was up to 79, and when in ice, algae are subject to a more stable and

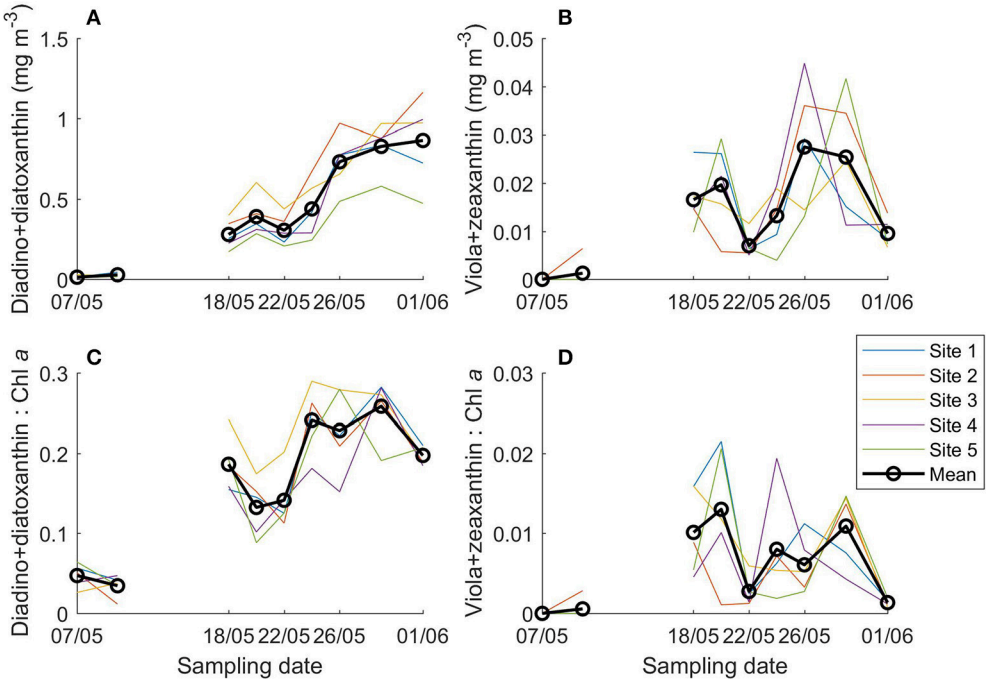

FIGURE 8 | Photoprotective xanthophyll cycle pigments concentration **(A,B)** and ratio to Chl *a* **(C,D)** in young ice during the ice coring transect study (7 May onwards).

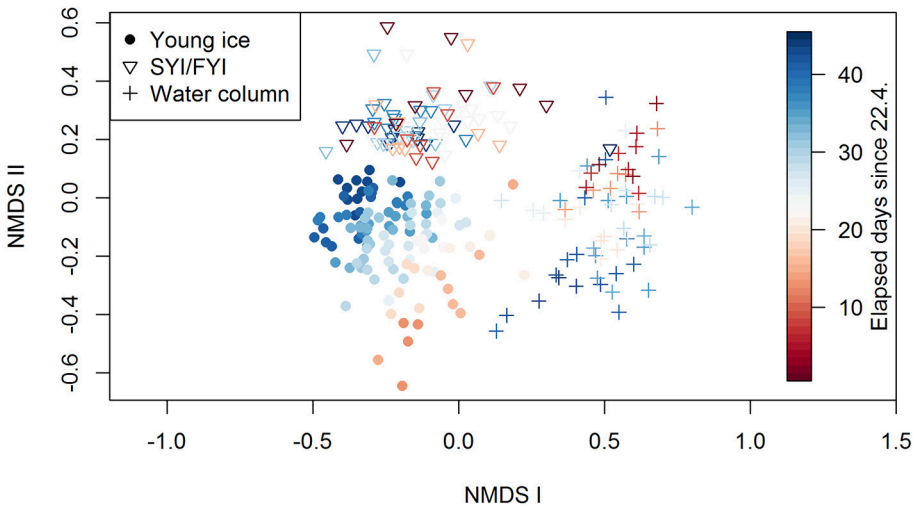

FIGURE 9 | Results of the NMDS analysis showing the grouping of young ice, SYI/FYI, and water column groups. The stress value of the plot is 16.6%.

intense light exposure than in the water column. Niemi et al. (2011) observed higher average number of taxa in new ice (1–6 days old) compared to older stages of ice (35+ days old), which could indicate that several species did not survive as the ice grew older. However, considering the long time gap other processes might have also played a role. Our water column taxonomy samples may also have missed the uppermost water layer, where the transport between ice habitats possibly occurs. Hardge et al. (2017) showed that the algal community at 1 m depth below ice was more similar to the deeper water column than to the FYI and MYI in the Central Arctic Ocean.

Separation of young ice from the SYI/FYI in the ordination (**Figure 9**) shows that the community in the young ice was not identical to the older ice. In the SYI/FYI group, no temporal patterns and thus succession was observed. In contrast, the young ice samples displayed a temporal trend in community composition, indicating that we were able to report the species succession in this habitat. The late young ice samples started to

resemble the SYI/FYI samples and became increasingly distinct from the water column samples, indicating that the young ice community evolved toward a more mature ice algal community.

This study indicates that surrounding ice is an important seeding source at a time of year when the water column has low algal, and especially low diatom, abundance. Ratkova and Wassmann (2005) observed that land-fast sea ice in the White Sea was dominated by pennate diatoms, whereas pack-ice communities in northern Barents Sea were dominated by flagellates, dinoflagellates and centric diatoms, pointing to the importance of sediments as another source for pennate diatoms. As Olsen et al. (2017b) suggest, MYI has an important role as a source in deep areas where the sediment repository is distant. Thus for the ice algal communities to mature to the typical pennate diatom community (Leu et al., 2015; van Leeuwe et al., 2018), contact with previous seasons' populations seems important, and in large parts of the Arctic, particularly the Central Basin, older ice likely plays a crucial role. This is further supported by the observations of Niemi et al. (2011), who found that the timing of ice formation did not determine the community composition in Cape Bathurst flaw lead in the Beaufort Sea, where new ice forms in leads throughout the winter and is surrounded by older first-year land-fast and pack ice. Two thirds of the taxa found in new ice (<6 days old) were not found in the water column but in older ice in their study. Even when phytoplankton is present during sea ice freezing in autumn, the sea ice community differs from the water column, showing that phytoplankton may not be the main source (Werner et al., 2007). In conclusion, timing of freezing (e.g., climate change caused later sea ice freezing in autumn) would be less important than proximity to sediments or older ice (i.e., existence of MYI) for the colonization of future ice algal assemblages.

Ice Algal Succession

From Ciliates and Flagellates to Pennate Diatoms

Biomass in the young ice increased over time but the species composition also changed considerably. On the first sampling days the protist community consisted mainly of ciliates, flagellates, and dinoflagellates, which gradually changed to dominance of pennate diatoms. The most prominent early colonizer of the young ice was the ciliate *M. rubrum*. Cryptophyte chloroplast symbionts of the ciliate (for review on the acquired phototrophy see Hansen et al., 2013) dominated in the young ice at the beginning of the study. *M. rubrum* was also found in the water column in the study region. The high abundance of the free symbionts is an artifact caused by disintegration of *M. rubrum* cells during sampling and fixation (Crawford, 1989), but it shows that *M. rubrum* was not limited to the under-ice water column but some cells also actively entered the ice. The symbionts contributed to a high concentration of the cryptophyte marker pigment alloxanthin, thus in this case alloxanthin indicates *M. rubrum* rather than free-living cryptophytes. The biomass of other cryptophytes was less than 6% of the symbiont biomass (not shown). In the first sampling days, alloxanthin had the highest marker pigment to Chl *a* ratios, confirming a high contribution of *M. rubrum* to the protist community.

The pigment gyroxanthin diester is usually associated with dinoflagellates and is also reported from one pelagophyte and two coccolithophore species (Table 14.2 in Johnsen et al., 2011). In the Arctic, it has previously been associated with the coccolithophore *Emiliana huxleyi* (Pettersen et al., 2011). In our samples, however, gyroxanthin diester seemed to be mainly associated with cryptophytes: temporal patterns of gyroxanthin diester were nearly identical to those of alloxanthin and α carotene, the marker pigments usually associated with cryptophytes (see **Figures 3E–G**, Supplementary Figures 3d–f). In contrast, neither pigments found in dinoflagellates (peridinin, dinoxanthin), pelagophytes (19′-butanoyloxyfucoxanthin; but-fuco), or haptophytes (Chl c_3 found for example in coccolithophores) had similar patterns to gyroxanthin diester. Moreover, Chl c_3 was only found in ice core top sections, whereas gyroxanthin diester only occurred in bottom sections (after ice core sectioning started), which shows that these two pigments were not co-located. Considering that most of the cryptophyte biomass originated from the *M. rubrum* symbionts, gyroxanthin diester seems to be associated with the cryptophyte-*M. rubrum* complex. In the samples where alloxanthin was present but gyroxanthin diester was not, other cryptophytes could be the alloxanthin source. This new observation has implications for using this pigment as an indicator for toxic dinoflagellates or *E. huxleyi* (Pettersen et al., 2011), but more studies are needed to confirm the findings.

Besides *M. rubrum*, dinoflagellates were initially important in the young ice. In terms of marker pigment to Chl *a* ratios, peridinin-containing dinoflagellates were relatively as important in the beginning of the transect sampling as fucoxanthin containing algae (e.g., diatoms) at the end of the study. Fucoxanthin is considered to originate mainly from diatoms because the microscopy analysis confirmed the high abundance of diatoms and another source of fucoxanthin, haptophytes, can be considered to be of minor importance due to the low concentration of the associated pigment Chl c_3. Dinoflagellates have been shown to increase in a post-bloom situation in FYI (Alou-Font et al., 2013) but our study shows that they can also contribute substantially to the young ice community at the beginning of its formation when the total algal biomass in the ice is still low. Total biomass of diatoms was much higher at the end of the study period than the initial dinoflagellate biomass. Diatom biomass was low at the beginning and mainly formed by centric diatoms, but from mid-May diatoms had a higher contribution to biomass than dinoflagellates and the fucoxanthin to Chl *a* ratio also increased over the sampling period. Centric diatoms were not very abundant (Supplementary Figure 2a), and throughout the sampling less abundant than pennate diatoms, but because of their relatively high biomass per cell they were prominent in biomass time series. At the end of the sampling, pennate diatoms clearly dominated also in terms of biomass and in the ice core top sections. The successional patterns are summarized in **Figure 10**. The group composition of the ice algal community is also reflected in the algal absorption spectra (Kauko et al., 2017 their Figure 3). The shoulders in the absorption spectra at 460 and 490 nm, caused by carotenoids and chlorophylls c_1 and c_2,

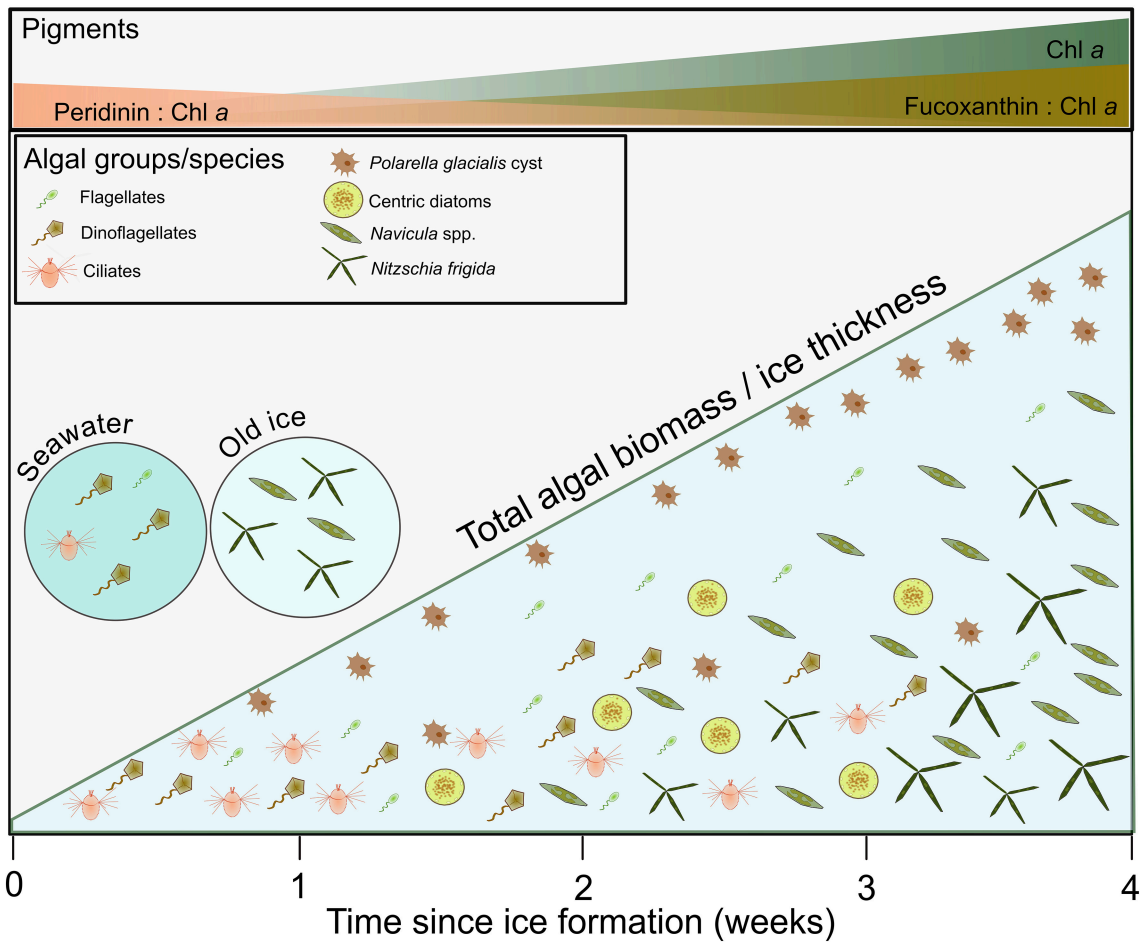

FIGURE 10 | A schematic showing the main successional patterns in the young ice and species composition in the source habitats old ice (i.e., SYI) and seawater (circles on the left). At the beginning, the young ice community had low biomass and was characterized by ciliates, dinoflagellates, and flagellates. Over a month, it developed toward dominance of pennate diatoms (especially *Navicula* spp. and *Nitzschia frigida*). Pennate diatoms eventually dominated also over centric diatoms. Cysts of *Polarella glacialis* were predominantly found in the top layer of the ice. Biomass in the bottom of the ice was typically higher than in the top part (coarsely indicated by the amount of icons within the young ice triangle), and increased over time (the diagonal line represents both increase in biomass and ice thickness in the young ice). In top panel the main patterns of algal marker pigment to Chl *a* ratios are shown, which show the succession from dinoflagellates (type I, peridinin) to diatoms (fucoxanthin).

and the exact wavelength of the *in vivo* red peak of Chl *a* (672–674 nm) are typical for diatoms and dinoflagellates (Johnsen and Sakshaug, 2007).

Chl *b* was the most prominent of the flagellate marker pigments, in addition to the cryptophyte pigments mentioned earlier. In our study Chl *b* likely originated mainly from prasinophytes since they were more abundant and frequent than chlorophytes based on microscopy counts (euglenophytes were not observed). Both based on biomass and low marker pigment concentrations (neoxanthin and lutein), these groups were rare. A fraction of the flagellate group was probably heterotrophic and therefore did not contribute to the marker pigments concentrations, which would also explain why dinoflagellates were relatively more prominent in pigment than count data in the early sampling period. Flagellate abundance could have been underestimated due to the unbuffered melting method used in this study (Garrison and Buck, 1986), but the concomitantly low flagellate marker pigment concentrations also indicate that they had a minor contribution to the ice algal biomass in the young ice, given that chloroplasts are retained on the sample filter.

Species succession from flagellates to diatoms was also observed over a few months in a mesocosm experiment where sea ice was formed from artificial sea water enriched with brine collected in Fram Strait (Weissenberger, 1998). Rózanska et al. (2008) observed that pennate diatoms were more abundant than centric diatoms or dinoflagellates in young ice (0.17–0.21 m thick) formed in fall in the Beaufort Sea, whereas the opposite was observed for new ice and nilas (thickness <0.08 m). Likewise,

Hegseth (1992) observed a succession from centric to pennate diatoms by studying pack ice floes of different age in Barents Sea, but the age of the different floes differed more than the time span of our sampling period. In some studies, however, new ice was already dominated by pennate diatoms (Okolodkov, 1992; Niemi et al., 2011) or centric diatoms became more abundant than pennates over the growth season (Galindo et al., 2017; Campbell et al., 2018). In general, pennate diatom dominance is a main succession stage during blooming bottom ice algal communities (Leu et al., 2015; van Leeuwe et al., 2018).

Cyst Formation

Cyst or resting stage formation are a part of the life cycle of many algae and are among others an adaptation to survive variable environmental conditions (Von Dassow and Montresor, 2011). In our study, cysts of the dinoflagellate *Polarella glacialis* and statocysts of the chrysophyte *Dinobryon* sp. were more abundant in the ice core top sections than in the bottom sections. The higher abundance of cysts from these groups in the upper ice was also found in previous studies (Stoecker et al., 1992, 1997; Garrison and Close, 1993; Gradinger, 1999; Werner et al., 2007). The cyst abundance and biomass increased over the sampling period, whereas vegetative cells were observed to a far lesser extent. This suggest that these species, after a short growth period in the ice, respond with rapid encystment. The pattern was observed throughout the entire sampling period, which means that algae encyst at the top of the ice core already before the main melting season in spring. This encystment seems to have occurred somewhat earlier than in studies from Antarctica (Stoecker et al., 1992; Garrison and Close, 1993), however, conditions in the young ice with thin snow cover and high irradiance may resemble a melting ice environment thus triggering encystment. The strong increase of *P. glacialis* cysts on the two last sampling days could also be a response to ice melt (ice thickness decreased). This encystment pattern over the whole period may however suggest that cysts are used as a dispersion strategy in addition to overwintering, as suggested by Stoecker et al. (1998). Inhabiting the ice surface would maximize dispersal distance, as that is the most likely part to survive longest and travel furthest. The mechanism to seek the surface could simply be controlled by light, as light intensity is higher further up in the ice. Cysts do not seem to have active Chl *a* (Stoecker et al., 1997) and presumably the photosynthetic apparatus is reduced, which explains the decline in peridinin concentration in our samples (**Figure 3C**) although biomass of the *P. glacialis* cysts increased (**Figure 5B**), and that peaks in dinoflagellate biomass and peridinin concentration do not always match (for *P. glacialis* pigments see Thomson et al., 2004). Thus for understanding survival strategies of sea ice biota, microscopic observations are important.

Species Diversity

Species richness increased over time in all habitats, and cumulative species number (Supplementary Figure 11) showed that the young ice community did not reach a plateau in species richness (if only species that were found on all days after they appeared were taken into account). In the ice habitats there were however no clear diversity changes over time (after removal of the symbionts) despite the increase in species richness. Shannon's diversity index indicates how difficult it is to predict the identity of a specimen taken randomly from the community, and Pielou's evenness describes how similar the abundances of the different species are (Peet, 1974), thus both species richness and evenness affect diversity. The low diversity indices and species evenness in the water column co-occur with the *P. pouchetii* under-ice bloom (Assmy et al., 2017b). The diversity pattern in the young ice case can be explained by the decrease in the species evenness: there are more species present, but some also become more dominant. Furthermore, in SYI the dominance seems to be stronger, because of lower evenness (and diversity) than in young ice or FYI. Thus ice algal communities seem to move in the course of succession toward lower diversity because of lower evenness at least during the bloom season. Alou-Font et al. (2013) observed that diversity did not vary between FYI sites with different snow cover (and thus light), but was lowest during peak bloom and highest during post bloom. MYI seems however to be important for the ice algal diversity: in a molecular study in Central Arctic Ocean, highest proportions of unique taxa (unique to ice as compared to melt ponds and water column) were found in MYI (Hardge et al., 2017). Compared to other studies of newly formed ice (that had less frequent sampling events than this study), the number of taxa was much higher in our case, spring young ice (120 taxa and 80 species), than in Beaufort Sea in autumn new ice ($\leq$6 days old; 46 taxa and 21 species; Niemi et al., 2011) or in autumn new ice, nilas, and young ice (ice thickness $\leq$ 0.21 m; 32–48 taxa and 18–26 species; Rózanska et al., 2008).

Drivers of Ice Algal Succession in Young Ice

In the young ice, there was a clear species succession as seen both in biomass and pigment concentration and also in the NMDS analysis. The main abiotic factors did not explain the variation in ice algal abundance to a great degree (17% of variation accounted for in constrained ordination; Supplementary Figure 10). Thus irradiance (indicated by snow thickness) does not seem to be a strong controlling factor of species succession. The significant correlation of bulk salinity with the unconstrained ordination (NMDS) is likely affected by the clear temporal patterns of bulk salinity caused by desalinization of the ice (Figure 2 in Kauko et al., 2017). The alignment of the first axis (in both ordinations) with the temporal gradient in the samples indicates that the main axis, along which the community varies is a temporal axis. Likewise, the correlation of water column nitrate with bulk salinity is likely caused by the temporal patterns, including strong nitrate drawdown during the under-ice phytoplankton bloom encountered in the latter half of the sampling period (Assmy et al., 2017b). Furthermore, bulk ($<$15; $<$9 during transect sampling) or brine salinities ($<$79; $<$52 during transect sampling) were not extreme in the young ice (this study and Kauko et al., 2017). Absence of grazing marker pigments (e.g., phaeophorbide *a*) indicate low grazing pressure. This and the weak control by the abiotic factors included here suggest that biotic factors, and moreover species traits and interactions advantageous for the sea ice environment, were likely important in community development (see Section Adaptation to Environmental Conditions and Morphology). This

conclusion is consistent with that the general pattern of diatom dominance (particularly pennate diatoms) in sea ice is similar across the Arctic (Poulin et al., 2011; Leu et al., 2015), despite a wide range in environmental conditions.

Irradiance

It should be noted that irradiance levels in our young ice case (on average 114 and range 30–350 μmol photons m^{-2} s^{-1}) were relatively high throughout the study period (Kauko et al., 2017). Light has been observed to impact community composition when experimentally perturbed (Enberg et al., 2015) or under different snow cover (Rózanska et al., 2009; Alou-Font et al., 2013). Alou-Font et al. (2013) observed no dinoflagellates under thick snow cover (lower light), but in our case they were found in both ice types. It has been suggested that higher abundance of centric compared to pennate diatoms in sea ice was due to higher light availability (Majaneva et al., 2017; Campbell et al., 2018). Exclusion of UV radiation led to biomass increase of *N. fridiga* in experiments (Enberg et al., 2015). In our samples, however, pennate diatoms dominated toward the end also in the young ice and in ice core top sections, i.e., under high irradiance. Thus in our study, this comparison, in addition to the statistical analysis, does not point to an important role of light in terms of community composition.

Nevertheless, photoacclimation is needed for the algae to be able to colonize new ice in spring. High irradiance can inhibit growth in non-acclimated cells (Mangoni et al., 2009; Juhl and Krembs, 2010). On the other hand, high irradiance likely enables more rapid growth in acclimated communities and dispersion in the ice in spring than in autumn. Ice algae have been considered to be highly shade adapted (Thomas and Dieckmann, 2002) and they can grow in very low light (<0.17 μmol photons m^{-2} s^{-1}; Hancke et al., 2018). Detailed studies on the photoacclimation capacities of ice algae conclude however that they have high plasticity regarding growth irradiance, aided to a large degree by the photoprotective xanthophyll cycle (Robinson et al., 1997; Petrou et al., 2011; Galindo et al., 2017). In our study, the xanthophyll cycle pigments diadino- and diatoxanthin showed an increasing trend both in concentration and ratio to Chl *a*, and thus show a response to increasing irradiance levels (Kauko et al., 2017 and Supplementary Figure 12). Diadino- and diatoxanthin are found in for example diatoms, dinoflagellates, and haptophytes (see Table 11.1 in Brunet et al., 2011) and thus represent the photoprotective mechanism of the majority of algae found in our samples. Other xanthophyll cycle pigments (violaxanthin and zeaxanthin, found e.g., in chlorophytes) were detected in our samples but in low concentrations and with a variable pattern, reflecting the low biomass of these algae in the samples in addition to the light exposure history. A similar seasonal increase in the photoprotective pigment pool in ice algae was also observed in FYI in the Canadian Arctic (Alou-Font et al., 2013; Galindo et al., 2017). The diadinoxanthin + diatoxanthin to Chl *a* ratios in our samples were in the range of what has been previously reported for surface habitats (ponds and slush) on Antarctic sea ice (Arrigo et al., 2014) or under thin snow cover in the Arctic (Alou-Font et al., 2013; Galindo et al., 2017). The average ratio was however similar in the surrounding FYI (data now shown) with much lower light levels [E_d(PAR) 1–20 μmol photons m^{-2} s^{-1}] than in the young ice (Olsen et al., 2017b). The ratios found in surrounding SYI [E_d(PAR) <1 μmol photons m^{-2} s^{-1}] were on average lower and similar to those in interior and bottom ice habitats in Arrigo et al. (2014).

The photoprotective pigment to Chl *a* ratios were not significantly different between the ice core top and bottom sections despite higher light exposure in the former. Based on radiative transfer modeling for 26 May (Kauko et al., 2017), the E_d(PAR) difference between the bottom and top 0.01 m of ice was >450 μmol photons m^{-2} s^{-1}. Alou-Font et al. (2013) found differences in photoprotective pigment to Chl *a* ratios already for irradiance levels of 26 and <10 μmol photons m^{-2} s^{-1} (between different snow covers). In our case the surrounding thick SYI had diadino- + diatoxanthin to Chl *a* ratios that were significantly lower in the bottom 0.20 m of the ice column, despite thick snow cover and thus high light attenuation also at the top of the ice column. These seemingly contradictory results suggest that the photoprotective pigment expression is controlled by more factors than purely light intensity, or that in many cases the expression is not fine-tuned but rather responds to broad categories or thresholds in light intensity (consider also the similarity between young ice and FYI in our case), or temporally integrated doses. When it comes to the photosynthetic pigments in our samples, differences between the young ice sections were again visible. Fucoxanthin to Chl *a* and Chl c_2 to Chl *a* ratios (the most prominent light harvesting pigments in our samples) were higher in ice core bottom sections. In lower light, algae increase the amount of photosynthetic pigments to effectively harvest the available light (Brunet et al., 2011).

Adaptation to Environmental Conditions and Morphology

The succession of the ice algal community, from a flagellate-dinoflagellate to a diatom dominated community, and within the diatoms from centric to pennate diatoms, indicates that sea ice communities evolve toward a more ice-adapted species community over time during a bloom. This was also suggested by Syvertsen (1991), based on changes in ice algal community composition from the ice edge northwards in the Barents Sea, i.e., from younger to older ice. The temporal patterns thus can be affected by the traits of the different species. When ice is formed, the species composition reflects what was present in the water column at the time of ice formation. Over time, selection occurs based on adaptation to the conditions in the ice and competition between species. *N. frigida* with the arborescent colonies, and other pennate species with attaching and gliding capabilities, are well adapted to life in brine channels, which to a certain degree resemble benthic habitats. Furthermore, they are adapted to the growth conditions: for example *N. frigida* grows exponentially even at very low temperatures and high salinities (Aletsee and Jahnke, 1992). *Fragilariopsis* species were in experiments found to be more tolerant to high salinities than a chlorophyte species (Søgaard et al., 2011) and are known to produce antifreeze proteins (Bayer-Giraldi et al., 2010). Additional biotic factors might also play a role in species succession; abundance of *F. cylindrus* (formerly *Nitzschia cylindrus*) was observed to decrease in connection with parasitic infection in the Beaufort Sea (Horner and

Schrader, 1982). The exponential increase of the major pennate diatoms in our study indicates that the growth conditions were favorable for them. However, when the seeding stock is low, they and especially *N. frigida* needed time to become dominant even at close to maximum growth rates (Olsen et al., 2017b).

Dinoflagellates in general are not considered as typical ice algae, but the brine community in upper ice in Antarctic land-fast ice can be dominated by dinoflagellates (Stoecker et al., 1992). Stoecker et al. (1997) reported that dinoflagellates and chrysophytes excysted and started photosyntethizing under extreme conditions (in terms of salinity and temperature) in the upper ice layers early in the season. Stoecker et al. (1998) observed that as the ice warmed, flagellates were replaced by pennate diatoms also in the upper ice. Dinoflagellates seem to be outcompeted by diatoms in the lower parts of ice and during more favorable growth conditions, but some species have evolved capacities to survive and find a niche. Resting cysts are a major component of the life cycle of ice-associated dinoflagellates (see discussion and references in section Cyst formation).

The pennate diatom *F. cylindrus* was, in terms of cell counts, an important species and had an exponential apparent growth rate until 29 May. Thereafter cell numbers declined strongly, possibly due to melting of ice (ice thickness began to decrease), which may have flushed the cells out. The ribbon shaped colonies may not be as optimal for attaching to the ice matrix as e.g., colonies of *N. frigida*. Otherwise it is well-adapted: Petrou et al. (2012) studied the photophysiology of *F. cylindrus* under temperature and nutrient stress and noticed that cell division rates decreased under nitrogen depletion, but physiological changes allowed for greater photoprotective capacity and photosynthetic efficiency was maintained. *Fragiolariopsis* species are also prominent ice algal species throughout the Arctic (Leu et al., 2015). However, *F. cylindrus* (and other small diatoms) in Antarctica was observed in experiments to synthetize mycosporine-like amino acids (MAAs) only in trace amounts that were not sufficient for effective UV protection (Riegger and Robinson, 1997), which could be a competitive disadvantage compared to species with higher amounts of MAAs. Judging by the high MAA to Chl *a* ratios found in the young ice in our case (Kauko et al., 2017), algae were investing strongly in UV protection. Thus both physical changes in the ice (melting) as well as physiological reasons (UV protection) could be responsible for the decline in this species during the study period. Likewise, centric diatoms (morphology shown in **Figure 6D**) were possibly affected by ice melting at the end of the study period.

In summary, the ice algal succession in young ice appears to start in a stochastic manner and then follows patterns that are dependent on the traits of the species present, resulting in differential adaptation to the ice habitat and its conditions (different succession concepts reviewed in McCook, 1994). Initially, species are likely to arrive in ice in a relatively random order based on abundances in the water column, which again are based on proximity to suitable source habitats such as older ice and water column bloom status. Once in ice, traits that provide a competitive advantage in the ice habitat determine the success of species to further grow and spread. Since the diatoms that were found in our early young ice were rarely observed in the water column, it suggests that the relatively few cells that came into contact with the young ice were successful in inhabiting and growing in the ice. Facilitation of the later arrivals by the early colonizers (see Connell and Slatyer, 1977) could occur as biologically produced extracellular polysaccharide substances have been observed to change the microstructure of growing ice (Krembs et al., 2011). Some degree of inhibition of later arrivals by early colonizers could also occur based on nutrient consumption, and in some cases because of allelopathy.

CONCLUSIONS

Our study provides the first observations of algal species succession in newly formed sea ice in spring. By following the same ice floe over an extended period of time we could observe the species succession at a high temporal resolution. The ice algal community originated both from the underlying water column and surrounding older ice, pointing to the importance of older ice as a seeding source. The community developed from a more mixed community toward dominance by ice-adapted pennate diatoms such as *N. frigida*. Overall the succession seemed to be determined more by the traits of the species than by variable abiotic factors. The colonization of the high light environment of young ice in spring is further aided by photoprotective carotenoids. The main trends in community succession were revealed also with marker pigment concentrations, with a fucoxanthin to Chl *a* ratio (indicative of diatoms) increase from 0.04 to 0.27 over the sampling period and low flagellate marker pigment concentrations. The pigment approach misses, however, the species succession within diatoms due to similar pigments, and patterns in cyst biomass due to lack of active photosynthesis in cysts. Cysts dominated the dinoflagellate biomass (>60%) on the majority of the sampling days. Cysts of the dinoflagellate *P. glacialis* were predominantly found in the top layers of the ice and were more prominent than the vegetative cells already in early May, which points to an important role of ice as a cyst repository and suggests that cysts may be used as a dispersion mechanism. With the decline in Arctic sea ice cover, loss of MYI and as ice retreats further away from the shelves, dispersal of ice algal species may be compromised, which could lead to changes in the relative importance of the dominant ice algal species. Based on this and previous studies, the source of pennate diatoms in new ice often seems to derive from surface sediments or older ice, whereas the time of freezing or environmental conditions play a smaller role in determining the community composition. In conclusion, the springtime young-ice algal community developed in less than a month into a typical, pennate diatom dominated community, when surrounding older sea ice can act as a seeding source.

AUTHOR CONTRIBUTIONS

PA, PD, MG, and CM planned the field work; PA, PD, MG, CM, HK, LO, MF-M, and AP conducted the field work; HK and

LO worked up the taxonomy data and planned the study; IP analyzed and processed the HPLC samples and HK worked up the data with the help of GJ and CM; MF-M made the schematics; HK did the statistical analysis and wrote the manuscript, and all co-authors contributed to the final version.

FUNDING

The N-ICE2015 campaign was made possible by the N-ICE project, supported by the Centre of Ice, Climate and Ecosystems at the Norwegian Polar Institute. HK, LO, PA, PD, MG, CM, and GJ were supported by the Research Council of Norway project Boom or Bust (no. 244646). GJ was supported by the Research Council of Norway project AMOS (no. 223254). CM was supported by the Natural Sciences and Engineering Council of Canada Discovery grant. MG and AP were supported by the Research Council of Norway project STASIS (no. 221961) and by the Polish-Norwegian Research Program operated by the National Centre for Research and Development under the Norwegian Financial Mechanism 2009–2014 in the frame of Project Contract Pol-Nor/197511/40/ 2013, CDOM-HEAT. MF-M and PA were supported by the Program Arktis 2030 funded by the Ministry of Foreign Affairs and Ministry of Climate and Environment, Norway (project ID Arctic). IP was funded by the PACES (Polar Regions and Coasts in a Changing Earth System) program of the Helmholtz Association.

ACKNOWLEDGMENTS

We would like to thank the captains and crew of RV Lance, and fellow scientists on N-ICE2015 for assistance. We acknowledge Jozef Wiktor, Magdalena Rózanska-Pluta, and Agnieszka Tatarek from the Institute of Oceanology of the Polish Academy of Sciences for species identification and enumeration, N-ICE2015 snow/ice team for ice temperature data, Anja Rösel for organizing the ice stratigraphy work, Torbjørn Taskjelle and Stephen Hudson for work with the irradiance data, and Max König for providing the map. Data used in the study is available through the Norwegian Polar Data Centre (Assmy et al., 2017a; Olsen et al., 2017a).

SUPPLEMENTARY MATERIAL

The Supplementary Material for this article can be found online at: https://www.frontiersin.org/articles/10.3389/fmars.2018.00199/full#supplementary-material

REFERENCES

Aletsee, L., and Jahnke, J. (1992). Growth and productivity of the psychrophilic marine diatoms *Thalassiosira antarctica* Comber and *Nitzschia frigida* Grunow in batch cultures at temperatures below the freezing point of sea water. *Polar Biol.* 11, 643–647. doi: 10.1007/BF00237960

Alou-Font, E., Mundy, C. J., Roy, S., Gosselin, M., and Agustí. S. (2013). Snow cover affects ice algal pigment composition in the coastal Arctic Ocean during spring. *Mar. Ecol. Prog. Ser.* 474, 89–104. doi: 10.3354/meps10107

Arrigo, K. R., Brown, Z. W., and Mills, M. M. (2014). Sea ice algal biomass and physiology in the Amundsen Sea, Antarctica. *Elem. Sci. Anthr.* 2:28. doi: 10.12952/journal.elementa.000028

Arrigo, K. R., and van Dijken, G. L. (2015). Continued increases in Arctic ocean primary production. *Prog. Oceanogr.* 136, 60–70. doi: 10.1016/j.pocean.2015.05.002

Assmy, P., Duarte, P., Dujardin, J., Fernández-Méndez, M., Fransson, A., Hodgson, R., et al. (2017a). *N-ICE2015 sea ice biogeochemistry [Data set]*. Tromsø: Norwegian Polar Data Centre. doi: 10.21334/npolar.2017.d3e93b31

Assmy, P., Fernández-Méndez, M., Duarte, P., Meyer, A., Randelhoff, A., Mundy, C. J., et al. (2017b). Leads in Arctic pack ice enable early phytoplankton blooms below snow-covered sea ice. *Sci. Rep.* 7:40850. doi: 10.1038/srep40850

Bayer-Giraldi, M., Uhlig, C., John, U., Mock, T., and Valentin, K. (2010). Antifreeze proteins in polar sea ice diatoms: diversity and gene expression in the genus Fragilariopsis. *Environ. Microbiol.* 12, 1041–1052. doi: 10.1111/j.1462-2920.2009.02149.x

Brunet, C., Johnsen, G., Lavaud, J., and Roy, S. (2011). "Pigments and photoacclimation processes," in *Phytoplankton Pigments - Characterization, Chemotaxonomy and Applications in Oceanography*, eds S. Roy, C. A. L. Lewellyn, E. S. Egeland, and G. Johnsen (Cambridge: Cambridge University Press), 445–471.

Campbell, K., Mundy, C. J., Belzile, C., Delaforge, A., and Rysgaard, S. (2018). Seasonal dynamics of algal and bacterial communities in Arctic sea ice under variable snow cover. *Polar Biol.* 41, 41–58. doi: 10.1007/s00300-017-2168-2

Connell, J., and Slatyer, R. O. (1977). Mechanisms of succession in natural communities and their role in community stability and organization. *Am. Nat.* 111, 1119–1144.

Cox, G. F. N., and Weeks, W. F. (1986). Changes in the salinity and porosity of sea-ice samples during shipping and storage. *J. Glaciol.* 32, 371–375.

Crawford, D. W. (1989). *Mesodinium rubrum*: the phytoplankter that wasn't. *Mar. Ecol. Prog. Ser.* 58, 161–174. doi: 10.3354/meps058161

Dieckmann, G. S., Spindler, M., Lange, M. A., Ackley, S. F., and Eicken, H. (1990). "Sea ice. a habitat for the foraminifer *Neogloboquadrina pachyderma*? in sea ice properties and processes," in *Proceedings of the W. F. Weeks Sea Ice Symposium, CRREL Monograph 90-1*, eds S. F. Ackley and W. F. Weeks (Hanover, NH: Cold Regions Research Engineering Laboratory), 86–92.

Dupont, F. (2012). Impact of sea-ice biology on overall primary production in a biophysical model of the pan-Arctic Ocean. *J. Geophys. Res. Oceans* 117, 1–18. doi: 10.1029/2011JC006983

Edler, L., and Elbrächter, M. (2010). "The Utermöhl method for quantitative phytoplankton analysis," in *Microscopic and Molecular Methods for Quantative Phytoplankton analysis*, eds B. Karlson, C. Cusack, and E. Bresnan (Paris: Intergovernmental Oceanographic Commission of UNESCO), 13–20.

Enberg, S., Piiparinen, J., Majaneva, M., Vähätalo, A. V., Autio, R., and Rintala, J.-M. (2015). Solar PAR and UVR modify the community composition and photosynthetic activity of sea ice algae. *FEMS Microbiol. Ecol.* 91, 1–11. doi: 10.1093/femsec/fiv102

Fernández-Méndez, M., Katlein, C., Rabe, B., Nicolaus, M., Peeken, I., Bakker, K., et al. (2015). Photosynthetic production in the central Arctic Ocean during the record sea-ice minimum in 2012. *Biogeosciences* 12, 3525–3549. doi: 10.5194/bg-12-3525-2015

Galindo, V., Gosselin, M., Lavaud, J., Mundy, C. J., Else, B., Ehn, J., et al. (2017). Pigment composition and photoprotection of Arctic sea ice algae during spring. *Mar. Ecol. Prog. Ser.* 585, 49–69. doi: 10.3354/meps1239

Garrison, D. L., and Buck, K. R. (1986). Organism losses during ice melting: a serious bias in sea ice community studies. *Polar Biol.* 6, 237–239. doi: 10.1007/BF00443401

Garrison, D. L., and Close, A. R. (1993). Winter ecology of the sea-ice biota in Weddell sea pack ice. *Mar. Ecol. Ser.* 96, 17–31.

Gosselin, M., Levasseur, M., Wheeler, P. A., Horner, R. A., and Booth, B. C. (1997). New measurements of phytoplankton and ice algal production in the Arctic Ocean. *Deep. Res. Part II Top. Stud. Oceanogr.* 44, 1623–1644. doi: 10.1016/S0967-0645(97)00054-4

Gradinger, R. (1999). Vertical fine structure of the biomass and composition of algal communities in Arctic pack ice. *Mar. Biol.* 133, 745–754.

Gradinger, R., and Ikävalko, J. (1998). Organism incorporation into newly forming Arctic sea ice in the Greenland Sea. *J. Plankton Res.* 20, 871–886. doi: 10.1093/plankt/20.5.871

Granskog, M. A., Assmy, P., Gerland, S., Spreen, G., Steen, H., and Smedsrud, L. H. (2016). Arctic research on thin ice: consequences of Arctic sea ice loss. *Eos. Trans. AGU* 97, 22–26. doi: 10.1029/2016EO044097

Granskog, M. A., Fer, I., Rinke, A., and Steen, H. (2018). Atmosphere-ice-ocean-ecosystem processes in a thinner Arctic sea ice regime: the Norwegian young sea ICE (N-ICE2015) expedition. *J. Geophys. Res. Ocean* 123, 1586–1594. doi: 10.1002/2017JC013328

Hancke, K., Lund-Hansen, L. C., Lamare, M. L., Pedersen, S. H., King, M. D., Andersen, P., et al. (2018). Extreme low light requirement for algae growth underneath sea ice : a case study from Station Nord, NE Greenland. *J. Geophys. Res. Oceans* 123, 985–1000. doi: 10.1002/2017JC013263

Hansen, P. J., Nielsen, L. T., Johnson, M., Berge, T., and Flynn, K. J. (2013). Acquired phototrophy in *Mesodinium* and *Dinophysis* - a review of cellular organization, prey selectivity, nutrient uptake and bioenergetics. *Harmful Algae* 28, 126–139. doi: 10.1016/j.hal.2013.06.004

Hardge, K., Peeken, I., Neuhaus, S., Lange, B. A., Stock, A., Stoeck, T., et al. (2017). The importance of sea ice for exchange of habitat-specific protist communities in the Central Arctic Ocean. *J. Mar. Syst.* 165, 124–138. doi: 10.1016/j.jmarsys.2016.10.004

Hegseth, E. N. (1992). Sub-ice algal assemblages of the Barents Sea: species composition, chemical composition, and growth rates. *Polar Biol.* 12, 485–496.

Higgins, H. W., Wright, S. W., and Schlüter, L. (2011). "Quantative interpretation of chemotaxonomic pigment data," in *Phytoplankton Pigments - Characterization, Chemotaxonomy and Applications in Oceanography*, eds S. Roy, C. A. LLewellyn, E. S. Egeland, and G. Johnsen (Cambridge: Cambridge University Press), 257–313.

Hillebrand, H., Dürselen, C.-D., Kirschtel, D., Pollingher, U., and Zohary, T. (1999). Biovolume calculation for pelagic and benthic microalgae. *J. Phycol.* 35, 403–424. doi: 10.1046/j.1529-8817.1999.3520403.x

Horner, R., and Schrader, G. C. (1982). Relative contributions of ice algae, phytoplankton, and benthic microalgae to primary production in nearshore regions of the Beaufort Sea. *Arctic* 35, 485–503. doi: 10.14430/arctic2356

Itkin, P., Spreen, G., Cheng, B., Doble, M., Girard-Ardhuin, F., Haapala, J., et al. (2017). Thin ice and storms: a case study of sea ice deformation from buoy arrays deployed during N-ICE2015. *J. Geophys. Res. Ocean.* 122, 4661–4674. doi: 10.1002/2016JC012403

Jeffrey, S. W., Wright, S. W., and Zapata, M. (2011). "Microalgal classes and their signature pigments," in *Phytoplankton Pigments - Characterization, Chemotaxonomy and Applications in Oceanography*, eds S. Roy, C. A. LLewellyn, E. S. Egeland, and G. Johnsen (Cambridge: Cambridge University Press), 3–77.

Johnsen, G., Moline, M. A., Pettersson, L. H., Pinckney, J., Pozdnyakov, D. V., Egeland, E. S., et al. (2011). "Optical monitoring of phytoplankton bloom pigment signatures," in *Phytoplankton Pigments - Characterization, Chemotaxonomy and Applications in Oceanography*, eds S. Roy, C. A. LLewellyn, E. S. Egeland, and G. Johnsen (Cambridge, UK: Cambridge University Press), 538–581.

Johnsen, G., and Sakshaug, E. (2007). Biooptical characteristics of PSII and PSI in 33 species (13 pigment groups) of marine phytoplankton, and the relevance for pulse-amplitude-modulated and fast-repetition-rate fluorometry. *J. Phycol.* 43, 1236–1251. doi: 10.1111/j.1529-8817.2007.00422.x

Juhl, A. R., and Krembs, C. (2010). Effects of snow removal and algal photoacclimation on growth and export of ice algae. *Polar Biol.* 33, 1057–1065. doi: 10.1007/s00300-010-0784-1

Kauko, H. M., Taskjelle, T., Assmy, P., Pavlov, A. K., Mundy, C. J., Duarte, P., et al. (2017). Windows in Arctic sea ice: light transmission and ice algae in a refrozen lead. *J. Geophys. Res. Biogeosci.* 122, 1486–1505. doi: 10.1002/2016JG003626

Krembs, C., Eicken, H., and Deming, J. W. (2011). Exopolymer alteration of physical properties of sea ice and implications for ice habitability and biogeochemistry in a warmer Arctic. *Proc. Natl. Acad. Sci. U.S.A.* 108, 3653–3658. doi: 10.1073/pnas.1100701108

Krembs, C., Tuschling, K., and von Juterzenka, K. (2002). The topography of the ice-water interface - its influence on the colonization of sea ice by algae. *Polar Biol.* 25, 106–117. doi: 10.1007/s003000100318

Lange, B. A., Flores, H., Michel, C., Beckers, J. F., Bublitz, A., Casey, J. A., et al. (2017). Pan-Arctic sea ice-algal chl *a* biomass and suitable habitat are largely underestimated for multiyear ice. *Glob. Chang. Biol.* 23, 4581–4597. doi: 10.1111/gcb.13742

Lange, M. A. (1988). Basic properties of Antarctic sea ice as revealed by textural analysis of ice cores. *Ann. Glaciol.* 10, 95–101.

Leppäranta, M., and Manninen, T. (1988). The brine and gas content of sea ice with attention to low salinities and high temperatures. *Finnish Inst. Mar. Res. Intern. Rep.* 2, 1–14.

Leu, E., Mundy, C. J., Assmy, P., Campbell, K., Gabrielsen, T. M., Gosselin, M., et al. (2015). Arctic spring awakening–steering principles behind the phenology of vernal ice algal blooms. *Prog. Oceanogr.* 139, 151–170. doi: 10.1016/j.pocean.2015.07.012

Lund-Hansen, L. C., Hawes, I., Nielsen, M. H., and Sorrell, B. K. (2017). Is colonization of sea ice by diatoms facilitated by increased surface roughness in growing ice crystals? *Polar Biol.* 40, 593–602. doi: 10.1007/s00300-016-1981-3

Majaneva, M., Blomster, J., Müller, S., Autio, R., Majaneva, S., Hyytiäinen, K., et al. (2017). Sea-ice eukaryotes of the Gulf of Finland, Baltic Sea, and evidence for herbivory on weakly shade-adapted ice algae. *Eur. J. Protistol.* 57, 1–15. doi: 10.1016/j.ejop.2016.10.005

Mangoni, O., Carrada, G. C., Modigh, M., Catalano, G., and Saggiomo, V. (2009). Photoacclimation in Antarctic bottom ice algae: an experimental approach. *Polar Biol.* 32, 325–335. doi: 10.1007/s00300-008-0517-x

McCook, L. J. (1994). Understanding ecological community succession: causal models and theories, a review. *Vegetatio* 110, 115–147.

Meier, W. N., Hovelsrud, G. K., van Oort, B. E. H., Key, J. R., Kovacs, K. M., Michel, C., et al. (2014). Actic sea ice in transformation: a review of recent observed changes and impacts on biology and human activity. *Rev. Geophys.* 51, 185–217. doi: 10.1002/2013RG000431

Meiners, K., Gradinger, R., Fehling, J., Civitarese, G., and Spindler, M. (2003). Vertical distribution of exopolymer particles in sea ice of the Fram Strait (Arctic) during autumn. *Mar. Ecol. Prog. Ser.* 248, 1–13. doi: 10.3354/meps248001

Melnikov, I. A. (1995). An *in situ* experimental study of young sea ice formation on an Antarctic lead. *J. Geophys. Res.* 100, 4673–4680.

Menden-Deuer, S., and Lessard, E. J. (2000). Carbon to volume relationship for dinoflagellates, diatoms and other protist plankton. *Limnol. Oceanogr.* 45, 569–579. doi: 10.4319/lo.2000.45.3.0569

Meyer, A., Sundfjord, A., Fer, I., Provost, C., Villacieros Robineau, N., Koenig, Z., et al. (2017). Winter to summer oceanographic observations in the Arctic Ocean north of Svalbard. *J. Geophys. Res. Ocean.* 122, 6218–6237. doi: 10.1002/2016JC012391

Niemi, A., Michel, C., Hille, K., and Poulin, M. (2011). Protist assemblages in winter sea ice: setting the stage for the spring ice algal bloom. *Polar Biol.* 34, 1803–1817. doi: 10.1007/s00300-011-1059-1

Okolodkov, Y. B. (1992). Cryopelagic flora of the Chukchi, East Siberian and Laptev Seas. *Proc. NIPR Symp. Polar Biol.* 5, 28–43.

Oksanen, J., Blanchet, F. G., Friendly, M., Kindt, R., Legendre, P., McGlinn, D., et al. (2017). *Vegan: Community Ecology Package*. Available online at: https://cran.r-project.org/package=vegan

Olsen, L. M., Assmy, P., Duarte, P., Laney, S. R., Fernández-Méndez, M., Kauko, H. M., et al. (2017a). *N-ICE2015 Phytoplankton and Ice Algae Taxonomy and Abundance [Data set]*. Tromsø: Norwegian Polar Data Centre. doi: 10.21334/npolar.2017.dc61cb24

Olsen, L. M., Laney, S. R., Duarte, P., Kauko, H. M., Fernández-Méndez, M., Mundy, C. J., et al. (2017b). The seeding of ice algal blooms in Arctic pack ice: the multiyear ice seed repository hypothesis. *J. Geophys. Res. Biogeosci.* 122, 1–20. doi: 10.1002/2016JG003668

Peet, R. K. (1974). The measurement of species diversity. *Annu. Rev. Ecol. Syst.* 5, 285–307.

Petrich, C., and Eicken, H. (2010). "Growth, structure and properties of sea ice," in *Sea Ice*, eds D. N. Thomas and G. S. Dieckmann (Oxford, UK: Wiley-Blackwell), 23–77.

Petrou, K., Hill, R., Doblin, M. A., McMinn, A., Johnson, R., Wright, S. W., et al. (2011). Photoprotection of sea-ice microalgal communities from the east Antarctic pack ice. *J. Phycol.* 47, 77–86. doi: 10.1111/j.1529-8817.2010.00944.x

Petrou, K., Kranz, S. A., Doblin, M. A., and Ralph, P. J. (2012). Photophysiological responses of *Fragilariopsis cylindrus* (Bacillariophyceae) to nitrogen depletion at two temperatures. *J. Phycol.* 48, 127–136. doi: 10.1111/j.1529-8817.2011.01107.x

Pettersen, R., Johnsen, G., Berge, J., and Hovland, E. K. (2011). Phytoplankton chemotaxonomy in waters around the Svalbard archipelago reveals high amounts of Chl *b* and presence of gyroxanthin-diester. *Polar Biol.* 34, 627–635. doi: 10.1007/s00300-010-0917-6

Poulin, M., Daugbjerg, N., Gradinger, R., Ilyash, L., Ratkova, T., and von Quillfeldt, C. (2011). The pan-Arctic biodiversity of marine pelagic and sea-ice unicellular eukaryotes: a first-attempt assessment. *Mar. Biodivers.* 41, 13–28. doi: 10.1007/s.12526-010-0058-8

R Core Team (2017). *R: A Language and Environment for Statistical Computing*. Vienna: R Foundation for Statistical Computing. Available online at: https://www.R-project.org/

Ratkova, T. N., and Wassmann, P. (2005). Sea ice algae in the White and Barents seas: composition and origin. *Polar Res.* 24, 95–110. doi: 10.1111/j.1751-8369.2005.tb00143.x

Reimnitz, E., Kempema, E. W., Weber, W. S., Clayton, J. R., and Payne, J. R. (1990). "Suspended-matter scavenging by rising frazil ice," in *Sea Ice Properties and Processes, Proceedings of the W. F. Weeks Sea Ice Symposium, CRREL Monograph 90-1*, eds S. F. Ackley and W. F. Weeks (Hanover, NH: Cold Regions Research Engineering Laboratory), 97–100.

Riedel, A., Michel, C., Gosselin, M., and LeBlanc, B. (2007). Enrichment of nutrients, exopolymeric substances and microorganisms in newly formed sea ice on the Mackenzie shelf. *Mar. Ecol. Prog. Ser.* 342, 55–67. doi: 10.3354/meps342055

Riegger, L., and Robinson, D. (1997). Photoinduction of UV-absorbing compounds in Antarctic diatoms and *Phaeocystis antarctica*. *Mar. Ecol. Prog. Ser.* 160, 13–25. doi: 10.3354/meps160013

Rintala, J.-M., Piiparinen, J., Blomster, J., Majaneva, M., Müller, S., Uusikivi, J., et al. (2014). Fast direct melting of brackish sea-ice samples results in biologically more accurate results than slow buffered melting. *Polar Biol.* 37, 1811–1822. doi: 10.1007/s00300-014-1563-1

Robinson, D. H., Kolber, Z., and Sullivan, C. W. (1997). Photophysiology and photoacclimation in surface sea ice algae from McMurdo Sound, Antarctica. *Mar. Ecol. Prog. Ser.* 147, 243–256. doi: 10.3354/meps147243

Rösel, A., Itkin, P., King, J., Divine, D., Wang, C., Granskog, M. A., et al. (2018). Thin sea ice, thick snow and widespread negative freeboard observed during N-ICE2015 north of Svalbard. *J. Geophys. Res. Ocean* 123, 1–21. doi: 10.1002/2017JC012865

Roy, S., Lewellyn, C. A., Egeland, E. S., and Johnsen, G., (eds) (2011). *Phytoplankton Pigments - Characterization, Chemotaxonomy and Applications in Oceanography, 1st Edn*. Cambridge: Cambridge University Press.

Rózanska, M., Gosselin, M., Poulin, M., Wiktor, J. M., and Michel, C. (2009). Influence of environmental factors on the development of bottom ice protist communities during the winter-spring transition. *Mar. Ecol. Prog. Ser.* 386, 43–59. doi: 10.3354/meps08092

Rózanska, M., Poulin, M., and Gosselin, M. (2008). Protist entrapment in newly formed sea ice in the Coastal Arctic Ocean. *J. Mar. Syst.* 74, 887–901. doi: 10.1016/j.jmarsys.2007.11.009

Rysgaard, S., and Nielsen, T. G. (2006). Carbon cycling in a high-arctic marine ecosystem-Young Sound, NE Greenland. *Prog. Oceanogr.* 71, 426–445. doi: 10.1016/j.pocean.2006.09.004

Søgaard, D. H., Hansen, P. J., Rysgaard, S., and Glud, R. N. (2011). Growth limitation of three Arctic sea ice algal species: effects of salinity, pH, and inorganic carbon availability. *Polar Biol.* 34, 1157–1165. doi: 10.1007/s00300-011-0976-3

Søreide, J. E., Leu, E., Berge, J., Graeve, M., and Falk-Petersen, S. (2010). Timing of blooms, algal food quality and *Calanus glacialis* reproduction and growth in a changing Arctic. *Glob. Chang. Biol.* 16, 3154–3163. doi: 10.1111/j.1365-2486.2010.02175.x

Stoecker, D. K., Buck, K. R., and Putt, M. (1992). Changes in the sea-ice brine community during the spring- summer transition, McMurdo Sound, Antarctica. I. Photosynthetic protists. *Mar. Ecol. Prog. Ser. Ser.* 84, 265–278.

Stoecker, D. K., Gustafson, D. E., Black, M. M. D., and Baier, C. T. (1998). Population dynamics of microalgae in the upper land-fast sea ice at a snow-free location. *J. Phycol.* 34, 60–69. doi: 10.1046/j.1529-8817.1998.340060.x

Stoecker, D. K., Gustafson, D. E., Merrell, J. R., Black, M. M. D., and Baier, C. T. (1997). Excystment and growth of chrysophytes and dinoflagellates at low temperatures and high salinities in Antarctic sea-ice. *J. Phycol.* 33, 585–595. doi: 10.1111/j.0022-3646.1997.00585.x

Syvertsen, E. E. (1991). Ice algae in the Barents Sea: types of assemblages, origin, fate and role in the ice-edge phytoplankton bloom. *Polar Res.* 10, 277–288. doi: 10.1111/j.1751-8369.1991.tb00653.x

Taskjelle, T., Hudson, S. R., Pavlov, A. K., and Granskog, M. A. (2016). *N-ICE2015 Surface and Under-Ice Spectral Shortwave Radiation Data [Data set]*. Tromsø: Norwegian Polar Data Centre. doi: 10.21334/npolar.2016.9089792e

Thomas, D. N., and Dieckmann, G. S. (2002). Antarctic sea ice - a habitat for extremophiles. *Science* 295, 641–644. doi: 10.1126/science.1063391

Thomson, P. G., Wright, S. W., Bolch, C. J. S., Nichols, P. D., Skerratt, J. H., and McMinn, A. (2004). Antarctic distribution, pigment and lipid composition, and molecular identification of the brine dinoflagellate *Polarella glacialis* (Dinophyceae). *J. Phycol.* 40, 867–873. doi: 10.1111/j.1529-8817.2004.03169.x

Tran, S., Bonsang, B., Gros, V., Peeken, I., Sarda-Esteve, R., Bernhardt, A., et al. (2013). A survey of carbon monoxide and non-methane hydrocarbons in the Arctic Ocean during summer 2010. *Biogeosciences* 10, 1909–1935. doi: 10.5194/bg-10-1909-2013

Tuschling, K. V., Juterzenka, K., Okolodkov, Y. B., and Anoshkin, A. (2000). Composition and distribution of the pelagic and sympagic algal assemblages in the Laptev Sea during autumnal freeze-up. *J. Plankton Res.* 22, 843–864. doi: 10.1093/plankt/22.5.843

van Leeuwe, M. A., Tedesco, L., Arrigo, K. R., Assmy, P., Campbell, K., Meiners, K. M., et al. (2018). Microalgal community structure and primary production in Arctic and Antarctic sea ice: a synthesis. *Elem. Sci. Anthr.* 6:4. doi: 10.1525/elementa.267

Venables, W. N., and Ripley, B. D. (2002). *Modern Applied Statistics With S, 4th Edn*. New York, NY: Springer.

Von Dassow, P., and Montresor, M. (2011). Unveiling the mysteries of phytoplankton life cycles: patterns and opportunities behind complexity. *J. Plankton Res.* 33, 3–12. doi: 10.1093/plankt/fbq137

Weissenberger, J. (1998). Arctic Sea ice biota: design and evaluation of a mesocosm experiment. *Polar Biol.* 19, 151–159.

Weissenberger, J., and Grossmann, S. (1998). Experimental formation of sea ice: importance of water circulation and wave action for incorporation of phytoplankton and bacteria. *Polar Biol.* 20, 178–188. doi: 10.1007/s003000050294

Werner, I., Ikävalko, J., and Schünemann, H. (2007). Sea-ice algae in Arctic pack ice during late winter. *Polar Biol.* 30, 1493–1504. doi: 10.1007/s00300-007-0310-2

Conflict of Interest Statement: The authors declare that the research was conducted in the absence of any commercial or financial relationships that could be construed as a potential conflict of interest.